












## TECHNICAL ADVANCES AND RESOURCES

# Identification of HCMV-derived T cell epitopes in seropositive individuals through viral deletion models

Maren Lübke<sup>1</sup> , Stefanie Spalt<sup>1,2</sup> , Daniel J. Kowalewski<sup>1</sup> , Cosima Zimmermann<sup>3,4</sup> , Liane Bauersfeld<sup>3,4</sup>, Annika Nelde<sup>1,5</sup> , Leon Bichmann<sup>1,6</sup>, Ana Marcu<sup>1</sup> , Janet Kerstin Peper<sup>1</sup> , Oliver Kohlbacher<sup>6,7,8,9</sup>, Juliane S. Walz<sup>5</sup>, Vu Thuy Khanh Le-Trilling<sup>10</sup>, Hartmut Hengel<sup>3,4</sup> , Hans-Georg Rammensee<sup>1,2</sup> , Stefan Stevanović<sup>1,2</sup> , and Anne Helenius<sup>3,4</sup> 

**In healthy individuals, immune control of persistent human cytomegalovirus (HCMV) infection is effectively mediated by virus-specific CD4<sup>+</sup> and CD8<sup>+</sup> T cells. However, identifying the repertoire of T cell specificities for HCMV is hampered by the immense protein coding capacity of this betaherpesvirus. Here, we present a novel approach that employs HCMV deletion mutant viruses lacking HLA class I immunoevasins and allows direct identification of naturally presented HCMV-derived HLA ligands by mass spectrometry. We identified 368 unique HCMV-derived HLA class I ligands representing an unexpectedly broad panel of 123 HCMV antigens. Functional characterization revealed memory T cell responses in seropositive individuals for a substantial proportion (28%) of these novel peptides. Multiple HCMV-directed specificities in the memory T cell pool of single individuals indicate that physiologic anti-HCMV T cell responses are directed against a broad range of antigens. Thus, the unbiased identification of naturally presented viral epitopes enabled a comprehensive and systematic assessment of the physiological repertoire of anti-HCMV T cell specificities in seropositive individuals.**

## Introduction

Primary infection with human cytomegalovirus (HCMV) is followed by lifelong persistence with recurrent cycles of endogenous reactivation. The prevalence of HCMV in adults ranges from 40% to 90% and increases with age (Fülöp et al., 2013; Staras et al., 2006). While in the immunocompetent host, infection is usually controlled by an HCMV-specific immune response, severe damage is common in immunocompromised individuals. HCMV infection or reactivation is a major cause of morbidity and mortality in AIDS patients or transplant recipients, since CD8<sup>+</sup> but also CD4<sup>+</sup> T cell immunity plays a critical role in preventing lethal infection (Einsele et al., 2002; Quinnan et al., 1982; Reusser et al., 1991). Congenital infection of the fetus has considerable consequences involving the central nervous system, with sensorineural hearing loss, mental retardation, or even death. Further, it is thought that subclinical infections with HCMV are involved in a variety of diseases, for example certain

cancers and inflammatory, hypertensive, and pulmonary diseases (Harkins et al., 2002; Li et al., 2011; Söderberg-Nauclér, 2006, 2008; Zhou et al., 1996). Therefore, development of better therapies and prevention strategies is of considerable importance. Current HCMV treatments include antiviral drugs and attempts to exploit humoral and cellular immune responses. Furthermore, considerable effort is made on the development of an HCMV vaccine (Plotkin and Boppa, 2018). Deeper insights into potential target structures are vitally important for all immunologic therapies.

With its almost 236-kbp-long double-stranded DNA, HCMV has the largest genome among human herpesviruses. The majority of studies on cytotoxic T lymphocyte responses have thus been restricted to a very limited selection of HCMV antigens; most prominent among them are the immunodominant antigens pp65 and IE1 (Akiyama et al., 2002; Kern et al., 1999; Le Roy and

<sup>1</sup>Department of Immunology, Interfaculty Institute for Cell Biology, University of Tübingen, Tübingen, Germany; <sup>2</sup>German Cancer Consortium, Partner Site Tübingen, Tübingen, Germany; <sup>3</sup>Institute of Virology, Medical Center University of Freiburg, Freiburg, Germany; <sup>4</sup>Faculty of Medicine, University of Freiburg, Freiburg, Germany; <sup>5</sup>Department of Hematology and Oncology, University Hospital Tübingen, Tübingen, Germany; <sup>6</sup>Applied Bioinformatics, Center for Bioinformatics and Department of Computer Science, University of Tübingen, Tübingen, Germany; <sup>7</sup>Quantitative Biology Center, University of Tübingen, Tübingen, Germany; <sup>8</sup>Biomolecular Interactions, Max-Planck-Institute for Developmental Biology, Tübingen, Germany; <sup>9</sup>Institute for Translational Bioinformatics, University Hospital Tübingen, Tübingen, Germany; <sup>10</sup>Institute for Virology, University of Duisburg-Essen, Essen, Germany.

Correspondence to Maren Lübke: [maren.luebke@uni-tuebingen.de](mailto:maren.luebke@uni-tuebingen.de); S. Spalt's and D.J. Kowalewski's present address is Immatics Biotechnologies GmbH, Tübingen, Germany.

© 2019 Lübke et al. This article is distributed under the terms of an Attribution-Noncommercial-Share Alike-No Mirror Sites license for the first six months after the publication date (see <http://www.rupress.org/terms/>). After six months it is available under a Creative Commons License (Attribution-Noncommercial-Share Alike 4.0 International license, as described at <https://creativecommons.org/licenses/by-nc-sa/4.0/>).

Davignon, 2005; McLaughlin-Taylor et al., 1994; Wills et al., 1996). However, a number of studies have clearly demonstrated that the HCMV-specific T cell response targets a much broader spectrum of HCMV antigens (Elkington et al., 2003; Manley et al., 2004; Sylwester et al., 2005). To date, the identification of most HCMV-specific T cell targets has been based on prediction methods (Elkington et al., 2003; Hebart et al., 2002; Nastke et al., 2005) or the use of overlapping peptides (Sylwester et al., 2005). The approach of direct isolation of viral ligands from infected target cells, successfully used for some viral infections (Croft et al., 2019; Günther et al., 2015; McMurtrey et al., 2008; Meyer et al., 2008; Ternette et al., 2016), has been cumbersome due to strict control of peptide presentation by HCMV-encoded HLA class I (HLA-I) immunoevasins (Ahn et al., 1997; Furman et al., 2002; Gewurz et al., 2001; Hegde et al., 2002; Jones et al., 1996; Odeberg et al., 2003). Glycoproteins encoded by the *US6* gene family are able to impair the stability and localization of HLA-I. The glycoproteins *US2* and *US11* bind HLA-I molecules and mediate their retrotranslocation into the cytosol for subsequent degradation by the proteasome (Jones and Sun, 1997; Wiertz et al., 1996a,b). *US6* prevents the assembly of the HLA-I/peptide complexes by inhibiting the transport of peptides into the endoplasmic reticulum by the transporter associated with antigen processing (Ahn et al., 1997; Hewitt et al., 2001). The product of *US3* forms complexes with assembled  $\beta 2$ -microglobulin-associated HLA-I heavy chains, thereby blocking maturation and transport of HLA-I molecules to the cell surface (Jones et al., 1996).

We show for the first time that the use of HCMV gene deletion mutants lacking various immunoevasins enables the direct isolation and mass spectrometric identification of almost 370 HCMV-specific HLA-I peptide ligands eluted from 12 different HLA allotypes. Of these peptides, 28% induced memory T cell responses with multifunctional (IFN $\gamma$ , TNF, CD107a) effector functions in HCMV-positive donors. Finally, real-time cytotoxicity assays demonstrated highly effective cell lysis of HCMV-infected target cells by peptide-specific CD8 $^{+}$  T cell clones in vitro. These results confirm that viral HLA-I ligands eluted from infected fibroblast cell cultures reflect physiological peptide processing and presentation mechanisms and are able to induce immunity against HCMV. Therefore, these peptides present novel targets for the treatment of HCMV-associated diseases by antigen-specific immunotherapy.

## Results

### Deletion of HCMV-encoded immunoevasins rescues HLA-I expression of infected cells

So far, attempts to isolate naturally presented HCMV-derived HLA-I ligands have not been successful. The HCMV genome encodes for several immunoevasins targeting HLA-I at various stages of the antigen presentation pathway. Hence, we assumed that deletion of genes involved in HLA-I regulation would enable the direct identification of virally encoded HLA-I ligands. We constructed AD169VarL (with partial ULb' region; Le et al., 2011) deletion mutants lacking the genes *US2-6* ( $\Delta$ US2-6), *US2-6 + US11* ( $\Delta$ US2-6/*US11*), and *US2-11* ( $\Delta$ US2-11). To measure the level of

HLA-I rescue due to lack of specific immunoevasins, we infected two different fibroblast cell cultures expressing HLA-I types of interest: MRC-5 (HLA-A\*02:01, -A\*29:02, -B\*07:02, -B\*44:02, -C\*05:01, and -C\*07:02) and HF-99/7 (HLA-A\*01:01, -A\*03:01, -B\*08:01, -B\*51:01, -C\*01:02, and -C\*07:01). The rate of infection was controlled using Fc-FITC, which binds to HCMV-encoded Fc-receptors, and was proven to achieve at minimum 94% for MRC-5 and 88% for HF-99/7 cells (Fig. S1). At 48 h postinfection (h.p.i.), the HLA-I cell surface level was determined by flow cytometry using the pan-HLA-I antibody W6/32 (Fig. 1A). Interestingly, HLA-I down-regulation by AD169VarL wild-type virus varied strongly between fibroblasts. HLA-B\*44:02 is expressed at very low levels in mock-treated MRC-5 cells but is strongly induced in HCMV-infected cells (Zimmermann et al., 2019). This indicates that HLA-B\*44:02 might be responsible for the apparent lower level of reduction by AD169VarL compared with mock-treated cells. As expected, infection with HCMV mutant viruses lacking HLA-I immunoevasins exhibited a robust rescue of HLA-I at the cell surface, qualifying these virus mutants for subsequent HLA-I ligandome analysis of infected cells.

### Direct identification of HCMV-derived HLA-I ligands by mass spectrometry (MS)

In a first step, we performed MS analysis of immunoaffinity-purified peptide extracts isolated from MRC-5 cells to identify naturally processed and presented HCMV-derived HLA-I ligands. At 48 h.p.i., HLA-I ligands isolated from cells infected with AD169VarL ( $n = 1$ ),  $\Delta$ US2-6 ( $n = 3$ ),  $\Delta$ US2-6/ $\Delta$ US11 ( $n = 5$ ), and mock controls ( $n = 2$ ) were exhaustively analyzed by liquid chromatography-coupled tandem MS (LC-MS/MS) in three to seven technical replicates per sample. These MS analyses revealed 816 to 2,714 unique HLA ligands per sample (Fig. 1B). Only 3 of 816 (0.4%) of HLA ligands eluted from MRC-5 cells infected with AD169VarL wild-type virus were derived from HCMV, while infection with the deletion viruses resulted in substantially increased viral peptide identification rates and numbers. In MRC-5 cells infected with the mutant viruses  $\Delta$ US2-6 and  $\Delta$ US2-6/ $\Delta$ US11, 79 and 181 unique HCMV-derived HLA ligands were identified, respectively, resulting in a total number of 194 different viral peptides. Overlap analysis revealed 66 of 194 viral peptides to be presented on MRC-5 after infection with both deletion viruses (Fig. 1C). Interestingly, 13 of 79 (17%) and 114 of 181 (63%) viral peptides of  $\Delta$ US2-6 and  $\Delta$ US2-6/ $\Delta$ US11 infected cells, respectively, were unique. This demonstrates that the HLA-I immunoevasins affect not only the quantity, but also the quality of HLA-I antigen processing and presentation. Therefore, the use of varying HCMV deletion mutants can result in a higher variability of identified HCMV-derived peptide species. Furthermore, we isolated the HLA-presented peptides from several biological replicates for each infection to maximize the number of identified HCMV-derived peptides. Thereby, we were able to identify 37–63 (mean 51) unique viral HLA ligands on cells infected with  $\Delta$ US2-6, corresponding to 2.4–3.0% (mean 2.7%) of total HLA ligand identifications. Overlap analysis of viral ligands identified in the three independent HLA precipitations revealed 31 of 79 (39%) of peptides to be uniquely identified in a single

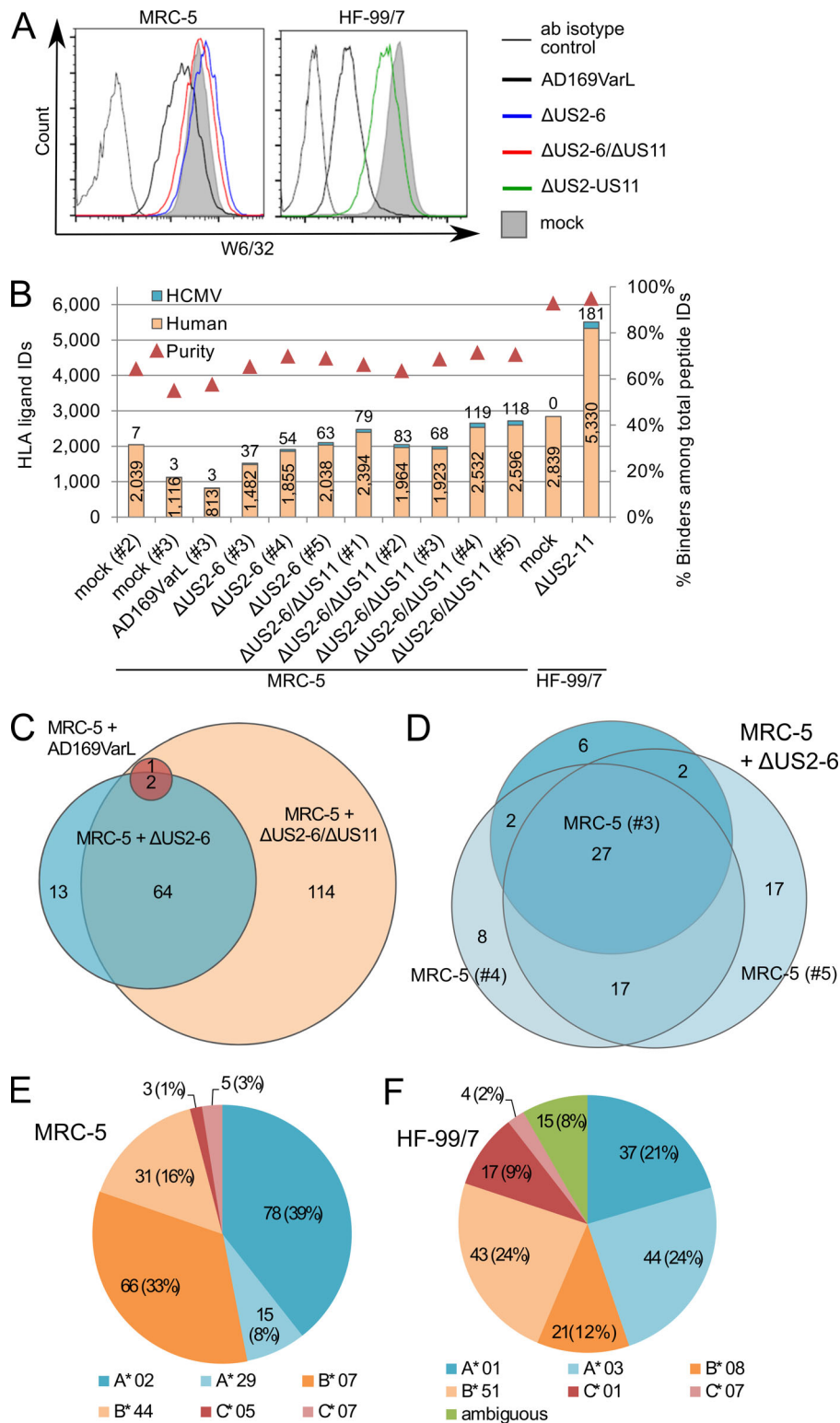


**Figure 1. Deletion of the genes *US2-11* allows identification of HCMV-derived HLA ligands from fibroblasts by LC-MS/MS. (A)** MRC-5 and HF-99/7 fibroblasts were mock-treated or infected with AD169VarL wild-type virus or deletion mutants with an MOI of 5. Cell surface expression of HLA-I (W6/32) was analyzed by flow cytometry at 48 h.p.i. Shown are representative results of two independent experiments. **(B)** Overview of HLA ligand identifications obtained by LC-MS/MS analysis of MRC-5 cells after mock treatment ( $n = 2$  independent experiments), infection with AD169VarL ( $n = 1$ ), and infection with the deletion viruses AD169  $\Delta$ US2-6 ( $n = 3$ ) or  $\Delta$ US2-6/ $\Delta$ US11 ( $n = 5$ ). Identified ligands of mock treated ( $n = 1$ ) or AD169  $\Delta$ US2-11 infected ( $n = 1$ ) HF-99/7 cells are depicted on the right side. Cells were infected with an MOI of 4–7. Peptide identifications were defined as HLA ligands if they showed predicted HLA binding defined as NetMHC IC<sub>50</sub>  $\leq$  500 nM and/or normalized SYF-PEITHI scores  $\geq$  50%. The purity of HLA ligand extracts (i.e., the ratio of predicted binders/total peptide identifications) of the individual HLA ligand elutions is indicated by red triangles. **(C)** Overlap analysis of the combined datasets of HCMV-derived HLA ligands identified on MRC-5 cells infected with the three different virus variants. **(D)** Overlap of HCMV-derived HLA ligands identified in three independent experiments using MRC-5 cells infected with the deletion virus  $\Delta$ US2-6. **(E and F)** Distribution of HLA restrictions among the 198 (MRC-5; E) and 181 (HF-99/7; F) unique HCMV-derived HLA ligands identified in total. Ab, antibody; IDs, identifications.

experiment, while 61% showed reproducible identification in at least two of three experiments (Fig. 1 D and Dataset S1). On cells infected with  $\Delta$ US2-6/ $\Delta$ US11, even higher proportions of viral ligands were identified, resulting in 68–119 (mean 93) unique viral HLA ligands corresponding to 3.2–4.5% (mean 3.9%) of total HLA ligands. Here, a similar degree of reproducibility was observed for the five independent precipitations, which resulted in

120 of 181 (66%) reproducible viral ligands (i.e., observed in at least two of the five experiments), while 61 of 181 (34%) were uniquely identified in individual experiments (Fig. S2). In total, immunopeptidome analyses of infected MRC-5 fibroblasts allowed the identification of 198 unique HCMV-derived HLA ligands, of which 78, 15, 66, 31, 3, and 5 are restricted to HLA-A\*02:01, -A\*29:02, -B\*07:02, -B\*44:02, -C\*05:01, and -C\*07:02,



respectively (Fig. 1 E and Dataset S1). Due to the applied 5% false discovery rate (FDR) in data processing, the identified 7 of 2,046 (0.34%) and 3 of 1,119 (0.27%) viral peptides in mock controls (Fig. 1 B) could be due to false-positive identifications. To estimate the actual FDR of HCMV-derived peptides, we compared fragment spectra of 50 randomly selected HLA-A\*02:01 and -B\*44:02-restricted synthetic peptides to their natural counterparts (Dataset S2). Fragmentation patterns matched for 48 of 50 (96%) spectrum pairs by manual validation, which is very consistent with the initially set FDR for a database search of 5%.

To extend the set of HCMV-derived ligands to additional HLA allotypes, we next infected primary human foreskin fibroblasts (HF-99/7) with the  $\Delta$ US2-11 deletion mutant. Peptide extracts from mock-treated ( $n = 1$ ) and infected cells ( $n = 1$ ) were analyzed in three LC-MS/MS runs, yielding 2,839 and 5,511 HLA ligands, respectively (Fig. 1 B). Of these, 37, 44, 21, 43, 17, and 4 viral peptides (altogether 181) were restricted to HLA-A\*01:01, -A\*03:01, -B\*08:01, -B\*51:01, -C\*01:02, and -C\*07:01, respectively (Fig. 1 F and Dataset S3). The HLA annotation of 15 peptides was ambiguous.

In total, 368 unique viral HLA-I ligands were identified from two different fibroblast cell cultures. Eleven ligands were found on both cell lines. We had speculated that an infection time of 48 h would allow the detection of peptides originating from proteins with various expression kinetics (Weekes et al., 2014). Indeed, the source proteins of the identified ligands represent all classes of gene expression (Datasets S1 and S3).

#### IFN $\gamma$ ELISpot screening validates numerous HCMV-derived ligands as T cell epitopes

All viral HLA-I ligands identified from MRC-5 cells and the top-ranked ligands from HF-99/7 cells ( $\geq 70\%$  SYFPEITHI score,  $\leq 50$  nM half-maximal inhibitory concentration [ $IC_{50}$ ], or  $< 0.5\%$  NetMHC percentile rank) were further evaluated for immunogenicity. Peptides were tested for memory T cell responses in at least seven different HCMV-seropositive HLA-matched individuals by IFN $\gamma$  ELISpot assay. HLA restriction and virus specificity of T cell responses were confirmed using HLA-mismatched and HCMV-seronegative donors as controls (not depicted). In total, 28% of all peptides elicited T cell responses in at least one individual (Table S1). This percentage was similar across all HLA restrictions (Fig. 2 A). Although we performed the ligandome analysis at only one time point after infection (48 h.p.i.), all temporal classes of viral gene expression (Weekes et al., 2014) were present among the source proteins of the identified epitopes (Fig. 2 B). As expected, normalized spot counts in IFN $\gamma$  ELISpot assays were donor dependent and in part highly variable (Figs. 2 C, S3, and S4). Based on the frequency of recognition, we grouped the peptides into three categories: negative (no memory response in any individual), subdominant (recognized by  $< 50\%$  of individuals), and dominant (recognized by  $\geq 50\%$  of individuals). Interestingly, in addition to the well-known epitopes derived from pp65, we were able to identify a number of other highly immunogenic peptides for each HLA restriction. Most immunogenic peptides, in proportion to the number of tested peptides, were found for HLA-A\*01:01,

whereas the highest proportion of dominant epitopes was found for HLA-B\*07:02 (Fig. 2 A).

We observed that for peptides with higher response rates, the average number of specific memory T cells after 12-d stimulation was often higher compared with peptides with lower recognition rates (Figs. 2 C and S3). To exclude the possibility of competitive effects among the different epitopes during the 12-d amplification, we additionally performed ex vivo IFN $\gamma$  ELISpots without prestimulation. Therefore, the dominant epitopes were retested with PBMC samples of previously tested positive donors. Only a few of the best epitopes elicited frequent, detectable responses ex vivo (Table 1). In most cases, memory T cell numbers were too small to be detectable ex vivo but underwent, in part, massive amplification ( $\leq 1,000$ -fold) upon prestimulation (Fig. 2 D). The amplification rate was highly individual for epitopes as well as for donors. In total, 103 HCMV-derived T cell epitopes were identified, of which 26 were shown to be dominant (Tables 1 and S1; and Fig. S5). These 26 dominant epitopes originate from 23 different proteins; three are derived from the well-known pp65 antigen (UL83). In case of positive results in HLA-mismatched ELISpot assays, the respective peptides were tested for the next-best predicted HLA-I allotype in ELISpot assays and/or for CD8 $^{+}$ /CD4 $^{+}$  T cell responses by intracellular cytokine staining (ICS). Three epitopes (UL147A<sub>2-10</sub>, UL34<sub>180-188</sub>, and UL26<sub>61-69</sub>) are potentially able to bind to more than one HLA-I allotype since they stimulated T cells of different donors harboring either of two well-predicted alleles. In addition to seven previously described epitopes (Table S1), six of them among the dominant epitopes, we were able to identify 96 novel HCMV-derived T cell epitopes. As we have previously observed (Nastke et al., 2005), ELISpot experiments revealed that HCMV-specific T cell responses are directed against a broad range of antigens within one donor; up to eight epitopes restricted by one specific HLA-I allotype were recognized in parallel (Fig. S4). While most donors, matching one distinct HLA allotype, showed responses to a similar set of epitopes restricted to this allotype (Fig. S4 A), some donors had highly individual patterns of recognition (Fig. S4 B).

#### HCMV-specific memory T cells are multifunctional

Peptide and HLA specificity of memory T cells was tested by HLA tetramer staining after 12-d amplification in vitro (Table 1 and Fig. 3 A). We were able to show distinct HCMV-specific CD8 $^{+}$  T cell populations for all but two (UL44<sub>259-267</sub> and UL150A<sub>152-161</sub>) dominant epitopes in several PBMC samples (Table 1). Specific T cell populations ranged from 0.3% to  $\leq 50\%$  after 12-d amplification. Functional activity of memory T cells after stimulation with HCMV peptides could be demonstrated by ICS via detection of IFN $\gamma$  and TNF (Fig. 3 B and Table 1). Predicted HLA restriction could be confirmed for 25 of 27 dominant epitopes. Stimulation with UL44<sub>259-267</sub> resulted in a T cell response mediated by CD4 $^{+}$  cells, while UL46<sub>76-84</sub> was able to activate CD4 $^{+}$  and CD8 $^{+}$  T cells in different PBMC samples. We assume that this activation of CD4 $^{+}$  T cells is specific and mediated by the presentation of those epitopes on HLA-II molecules. Coactivation of CD4 $^{+}$  T cells was never observed in ICS upon stimulation with our epitopes, and we hardly ever

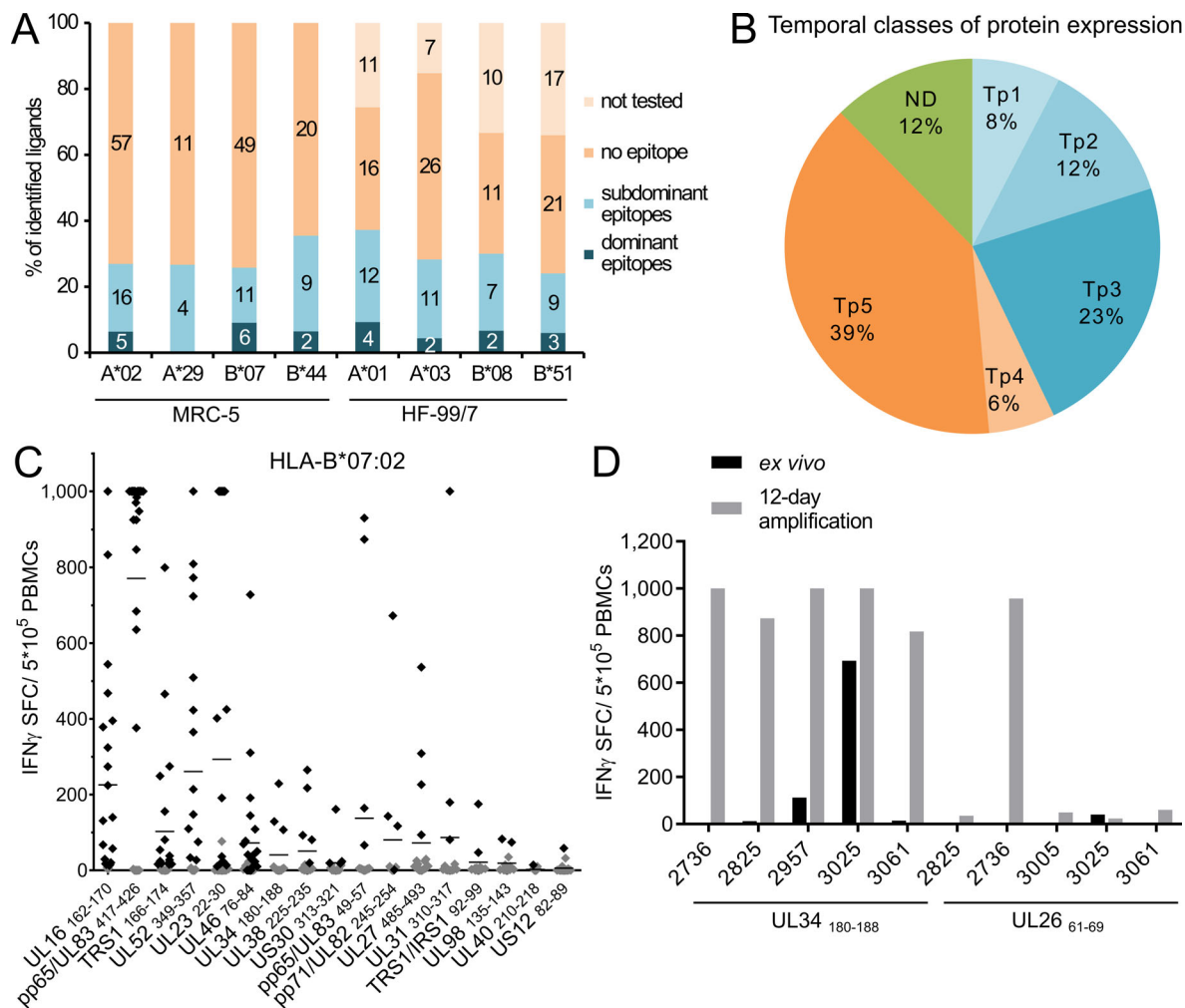


**Figure 2. Identification and characterization of naturally presented T cell epitopes by ELISpot assays.** HCMV ligands were tested for memory T cell response by IFN $\gamma$  ELISpot with PBMCs of healthy, seropositive donors. **(A)** Distribution of dominant and subdominant HCMV ligands restricted to HLA-A and -B allotypes. **(B)** Proportion of epitope source proteins assigned to five different temporal classes of protein expression according to [Weekes et al. \(2014\)](#). Source proteins not assigned to one of those classes are depicted as not determined (ND). **(C)** ELISpot screening results of positively tested HLA-B\*07:02-restricted peptides. Shown is the mean number of IFN $\gamma$  spot-forming cells (SFCs) from two technical replicates for each tested donor minus the mean spot number of the negative control of the respective donor. Spot counts of >1,000 were set to 1,000 because of inaccurate spot count due to technical limitations. Positively evaluated spot counts are depicted in black, and negatively evaluated spot counts in gray. **(D)** Comparison of IFN $\gamma$  SFC in ex vivo ELISpots (black) and ELISpots with prior 12-d amplification (gray). Shown are exemplary results of two independent experiments with five donors (coded by four-digit numbers) each for two B\*08 epitopes (UL34<sub>180-188</sub> and UL26<sub>61-69</sub>). ND, not determined.

detected unspecific activation of T cells in the negative controls of ELISpot assays and ICS. Furthermore, we could demonstrate that some epitopes elicit T cell responses restricted to more than one HLA-I allotype: T cell responses to UL26<sub>61-69</sub> were detected in HLA-B\*08<sup>+</sup>/B\*51<sup>-</sup> and HLA-B\*08<sup>-</sup>/B\*51<sup>+</sup> samples. In a following mismatch ELISpot with HLA-B\*08<sup>-</sup>/B\*51<sup>-</sup> donors, two HLA-B\*14<sup>+</sup> donors showed strong IFN $\gamma$  responses. ICS demonstrated that immune responses elicited by this epitope were mediated by CD8<sup>+</sup> T cells in all tested donors. Subsequent tetramer stainings verified HLA-B\*08, -B\*51, and B\*14 restriction of the epitope (Fig. 3 C). Further ELISpots with HLA-B\*14<sup>+</sup> donors revealed a recognition rate of 40%. In summary, we were able to further characterize dominant HCMV-derived epitopes using ICS, tetramer staining, and mismatch experiments.

#### HCMV-specific CD8<sup>+</sup> T cell clones effectively kill peptide-loaded or infected target cells

For examination of cytotoxic activity, CD8<sup>+</sup> T cell clones specific for UL23<sub>22-30</sub> (B\*07) were generated. Specificity and activity of the clones were assessed by HLA tetramer staining and ICS. T cell clones used for cytotoxicity experiments were highly specific and showed secretion of IFN $\gamma$  and TNF as well as expression of the degranulation marker CD107a (Fig. 4 A). To further characterize the cytotoxic potential of effector T cells, we applied the xCELLigence system. Without addition of HCMV-reactive CD8<sup>+</sup> T cells, the HCMV-infected MRC-5 cells displayed a specific cell index pattern as the infection proceeded and changed the cell morphology. A few hours after infection, MRC-5 cells started to round up and lose adherence to the plate as compared with mock-treated cells (Fig. S5 A). This is detected by

Table 1. Summary of dominant T cell epitopes

Protein	Sequence	Tested HLA	Actual HLA restriction	ELISpot response rate (%)		Intracellular staining	Tetramer staining
				12-d stimulation	Ex vivo (%) <sup>a</sup>		
pp65/UL83 <sub>495–503</sub>	NLVPMTATV <sup>b</sup>	A*02:01	A*02:01	75.0	100.0	CD8	Positive
US8 <sub>74–82</sub>	GVLDVWVRV	A*02:01	A*02:01	72.2	50.0	CD8	Positive
UL150A <sub>152–161</sub>	ALWDVALLEV	A*02:01	A*02:01	71.4	25.0	CD8	Positive
gM/UL100 <sub>200–208</sub>	TLIVNLVEV	A*02:01	A*02:01	55.0	25.0	CD8	Positive
UL44 <sub>259–267</sub>	GLFAVENFL	A*02:01	HLA-II	53.9	0.0	CD4	Not tested
UL16 <sub>162–170</sub>	YPRPPGSG <sup>b</sup>	B*07:02	B*07:02	86.4	25.0	Negative	Positive
pp65/UL83 <sub>417–426</sub>	TPRVTTGGAM <sup>b</sup>	B*07:02	B*07:02	81.6	100.0	CD8	Positive
TRS1 <sub>166–174</sub>	SPRDAWIVL	B*07:02	B*07:02	68.2	20.0	CD8	Positive
UL52 <sub>349–357</sub>	SPSRDRFVQL	B*07:02	B*07:02	66.7	33.3	Negative	Positive
UL23 <sub>22–30</sub>	RPWKPQGRV	B*07:02	B*07:02	53.6	66.7	CD8	Positive
UL46 <sub>76–84</sub>	SPRHLIYSL	B*07:02	B*07:02	50.0	0.0	CD4/CD8	Positive
UL112/ UL113 <sub>125–134</sub>	SEGNLQVTY	B*44:02	B*44:02	83.9	62.5	CD8	Positive
UL117 <sub>358–366</sub>	HETGVYQMW	B*44:02	B*44:02	65.4	62.5	CD8	Positive
UL105 <sub>715–723</sub>	YADPFLLKY <sup>b</sup>	A*01:01	A*01:01	100.0	90.9	CD8	Positive
UL44 <sub>245–253</sub>	VTEHDTLLY <sup>b</sup>	A*01:01	A*01:01	92.9	100.0	CD8	Positive
UL69 <sub>569–578</sub>	RTDPATLTAY	A*01:01	A*01:01	82.6	66.7	CD8	Positive
US28 <sub>122–130</sub>	ITEIALDRY	A*01:01	A*01:01	58.3	14.3	CD8	Positive
gB/UL55 <sub>657–665</sub>	NTDFRVLELY	A*01:01	A*01:01	56.3	0.0	CD8	Positive
UL77 <sub>228–236</sub>	GLYTQPRWK	A*03:01	A*03:01	76.2	50.0	CD8	Positive
UL57 <sub>790–798</sub>	RVKNRPIYR	A*03:01	A*03:01	60.9	33.3	CD8	Positive
UL34 <sub>180–188</sub>	LPHRHREL	B*08:01	B*08:01	90.9	85.7	CD8	Positive
UL26 <sub>61–69</sub>	LPYPRGYTL	B*08:01	B*08:01/51:01/14:02	68.8	16.7	CD8	Positive
UL13 <sub>465–473</sub>	YLVRPMTI	B*08:01	B*08:01	50.0	33.3	Negative	Positive
pp65/UL83 <sub>116–123</sub>	LPLKMLNI <sup>b</sup>	B*51:01	B*51:01	80.0	87.5	CD8	Positive
UL38 <sub>156–164</sub>	FPVEVRSHV	B*51:01	B*51:01	65.2	0.0	CD8	Positive
UL26 <sub>61–69</sub>	LPYPRGYTL	B*51:01	B*08:01/51:01/14:02	62.5	33.3	CD8	Positive
UL56 <sub>503–511</sub>	DARSRIHNV	B*51:01	B*51:01	53.3	20.0	CD8	Positive

<sup>a</sup>Ex vivo ELISpot assays were performed using donor samples that were positively tested in ELISpot assays with prior 12-d stimulation.

<sup>b</sup>Previously published epitope; references in Table S1.

a lower cell index in the xCELLigence system (Fig. S5 B). At approximately 20 h.p.i., cell indices increased again as MRC-5 cells started to readhere. Finally, the cell index dropped drastically 3–5 d after infection (depending on the applied multiplicity of infection [MOI]) due to cell lysis by the virus (Fig. S5 B). For optimal measurement of T cell-dependent cytotoxicity, effector T cells were added 48 h.p.i. This allowed recovery of the infected cells resulting in higher cell index values before late cell index drop due to infection. To test peptide specificity of the CD8<sup>+</sup> T cell clones, mock-treated MRC-5 cells were loaded with specific or unspecific peptides or infected with the  $\Delta$ US2-6 mutant, and effector cells were added in a 5:1 effector-to-target (E:T) cell ratio. Killing of peptide-loaded cells occurred very fast and was highly specific (Fig. 4 B); within 12 h almost all UL23<sub>22–30</sub>-loaded

target cells were killed by the specific T cell clone. Killing of  $\Delta$ US2-6-infected cells was delayed but equally efficient. Cell index values were much higher (indicating less cell lysis) for cells loaded with an unspecific or no peptide when cocultured with the UL23<sub>22–30</sub>-specific T cell clone. An E:T cell ratio-dependent killing of  $\Delta$ US2-6-infected MRC-5 cells started a few hours after addition of effector cells (Fig. 4 C) and reached 50% after 18 h (E:T cell ratio of 1:1 and higher). After 36 h (corresponding to 84 h.p.i.), almost all infected cells were killed by the peptide-specific CD8<sup>+</sup> T cell clones. Interestingly, despite the minimal expression of HLA-I loaded with viral peptides on the surface of AD169VarL-infected cells, a cytolytic effect was observed at higher E:T ratios, when normalized to infected cells without effector cells (Fig. 4 D). In accordance with the

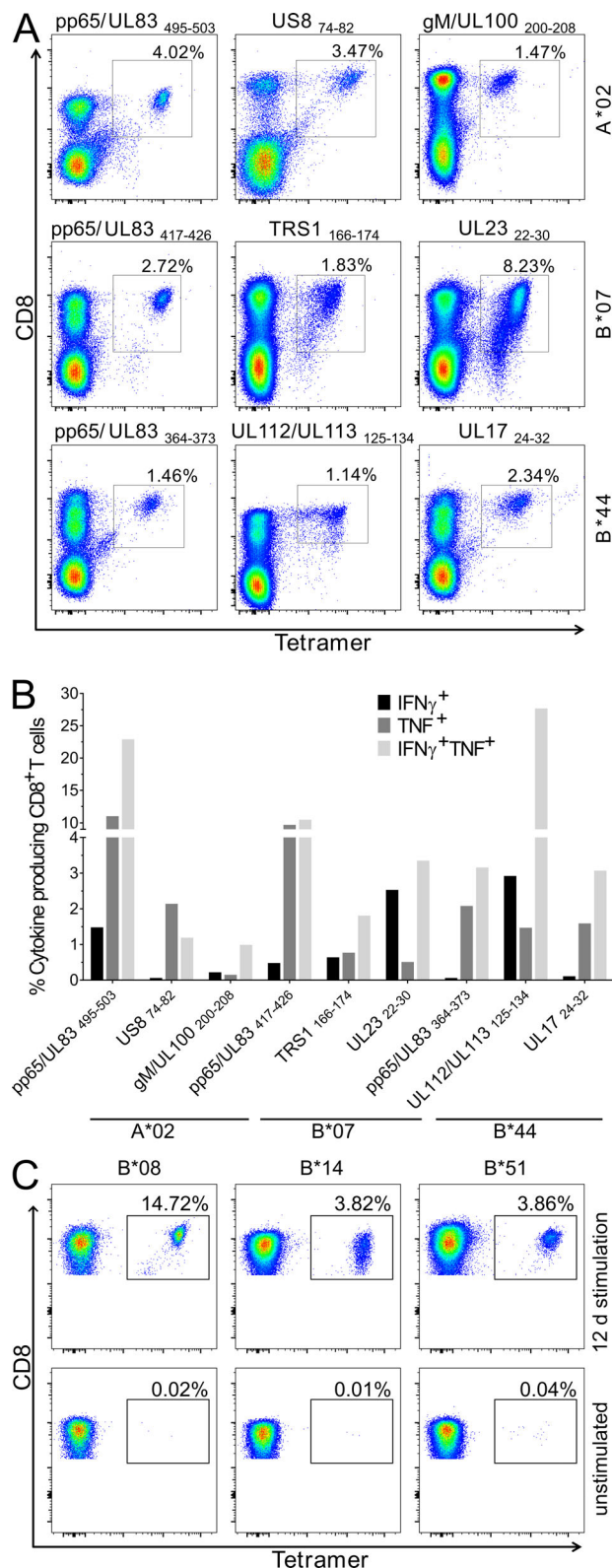


**Figure 3. Characterization of HCMV-specific memory T cells. (A)** Representative tetramer staining after 12-d in vitro amplification of CD8<sup>+</sup> T cells derived from HLA-matched healthy donors. Novel HCMV ligands are compared with known pp65 epitopes (left column). **(B)** Exemplary intracellular IFN $\gamma$  and TNF staining of healthy donor PBMCs after 12-d amplification measured by flow cytometry. Cells were stimulated with novel HCMV peptides or known pp65 epitopes. Bars represent percentage of CD8<sup>+</sup> T cells

assumption that low amounts of HLA-I/peptide complexes are responsible for the slow killing of AD169VarL-infected cells, the additional loading of specific peptide led to a dramatic increase of lysis (Fig. 4 D). Similar results were obtained with T cell clones specific for the HLA-B\*44-restricted dominant epitope UL112/UL113<sub>125-134</sub> (not depicted). The ability of T cell clones specific for newly identified epitopes to lyse not only peptide-loaded and mutant virus-infected but also wild-type virus-infected cells shows the great potential of those cytotoxic T cells. Together with the detected immune responses in healthy, seropositive donors, this confirms the involvement of HLA ligands derived from HCMV deletion mutants in physiologic immune control of HCMV infections.

### Comparison of in silico epitope prediction to MS HLA-I ligand identification

To compare our MS-based approach of identifying naturally presented epitopes with an established in silico prediction method, we applied the prediction tools SYFPEITHI and NetMHCpan3.0 to the proteome of HCMV. We ranked all peptides according to their prediction score and determined the position of our dominant epitopes within this dataset (Table S2). For both algorithms (SYFPEITHI and NetMHC), 25 of the 26 identified dominant epitopes are among the top-scoring 2% of all predicted peptides. This is in line with our previous experience that the top 2% of predicted peptides with SYFPEITHI usually contain the natural T cell epitopes (Rammensee et al., 1999). NetMHC categorizes its predicted peptides into weak (affinity <500 nM, % rank <2) and strong (affinity <50 nM, % rank <0.5) binders. Thus, it would be necessary to test ~1,300 (SYFPEITHI) or 2,000 (NetMHC) peptides for each HLA-I allotype and length variant to screen epitopes from the entire HCMV proteome within these thresholds. Furthermore, we sought to determine whether a correlation can be found between immunogenicity and HLA binding prediction that could improve the selection of peptide candidates in future studies. For this purpose, we exemplarily illustrated the rank of tested, HLA-A\*02-restricted 9mer peptides in the whole proteome prediction with SYFPEITHI against their immunogenicity (Fig. 5). We found a weak but significant negative correlation ( $\tau_b = -0.225$ ,  $P = 0.033$ ) between the prediction rank and the immunogenicity. Most dominant epitopes, but not all, are within the 2% candidates with the best prediction scores, and subdominant epitopes together with nonimmunogenic HLA-ligands also show widely dispersed prediction scores. Therefore, evidence of presentation on HLA molecules considerably reduces the number of possible candidates to be tested, as opposed to HLA binding prediction alone.

producing IFN $\gamma$  (black), TNF (gray), or both (light gray). Three peptides per HLA restriction, tested in one HLA-matched donor, are depicted. **(C)** Representative UL26<sub>61-69</sub> (LPYPRGYTL)-tetramer staining after 12-d in vitro amplification or no stimulation of CD8<sup>+</sup> T cells derived from HLA-matched healthy donors. Donor PBMCs (HLA-B\*08<sup>+</sup>, B\*14<sup>+</sup>, or B\*51<sup>+</sup>) were initially stimulated with UL26<sub>61-69</sub>. Staining was performed with UL26<sub>61-69</sub> tetramers specific for the respective HLA allotype. All tetramer stainings and ICS were performed once in two to four different donors per epitope.



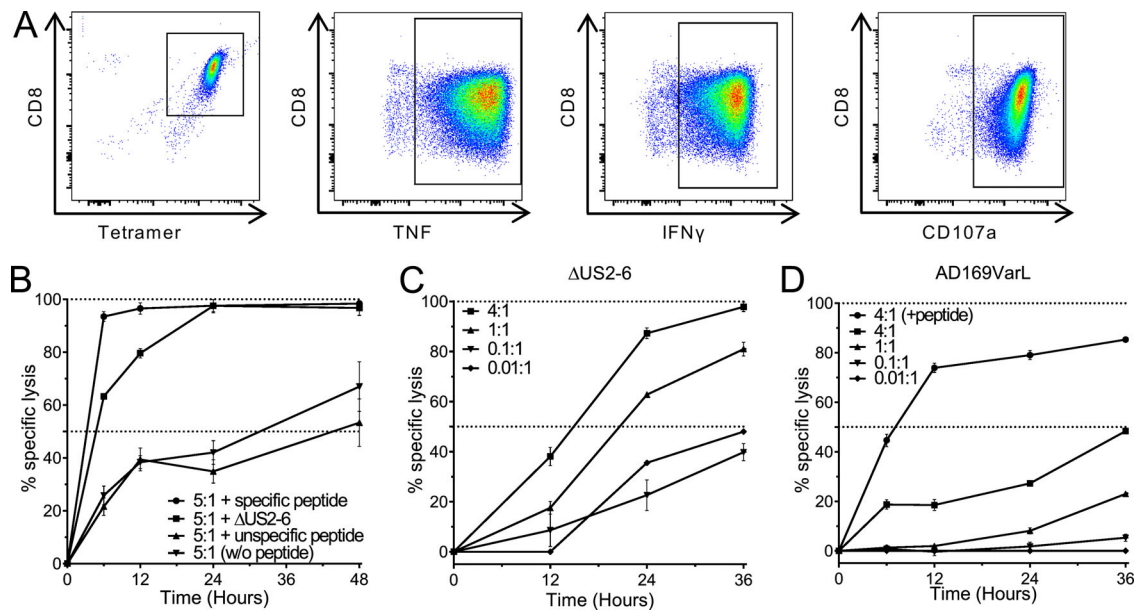


**Figure 4. Characterization and cytotoxicity of HCMV-specific CD8<sup>+</sup> T cell clones.** (A) Exemplary staining of a UL23<sub>22-30</sub>-specific T cell clone (B\*07:02-restricted) with the respective tetramer and ICS with TNF, IFN $\gamma$ , and the degranulation marker CD107a. Similar results were obtained with several clones per donors. (B–D) Real-time cytotoxicity of different UL23<sub>22-30</sub>-specific T cell clones monitored by the xCELLigence system. 20,000 cells/well of infected or mock-treated MRC-5 cells were seeded into 96-well E-plates. After attachment of target cells, effector cells were added 48 h.p.i. at indicated E:T ratios ( $t_0$ ). Synthetic peptides were added to target cells 1 h before effector cells. Percentage of lysis was calculated in relation to cells without effector T cells. Shown are representative results of three independent experiments. Error bars represent SD from technical triplicates. (B) MRC-5 cells were loaded with specific (UL23<sub>22-30</sub>, RPWKPQQRV) or unspecific (HIV Nef<sub>128-137</sub>, TPGPGVRYPL) peptide or infected with ΔUS2-6 (MOI 2) and incubated with effector cells in an E:T cell ratio of 5:1. MRC-5 cells without peptide served as a control. (C) Comparison of specific lysis of ΔUS2-6-infected MRC-5 cells with different E:T ratios. (D) Specific lysis of AD169VarL wild-type infected or peptide-loaded cells with indicated E:T cell ratios.

## Discussion

Various immune evasion strategies employed by HCMV strongly interfere with the HLA-I presentation of viral peptides on the host cell surface. However, ~10% of the memory T cell compartment of seropositive individuals consists of HCMV-specific

T cells (Sylwester et al., 2005), and this number can dramatically rise in elderly (Vescovini et al., 2007).

With our approach, we were able to bypass immune evasion by the US6 family genes and, for the first time, perform the direct isolation and identification of physiologically relevant HCMV-specific HLA ligands by MS. Our data clearly confirm that memory T cell responses toward peptides derived from viral proteins of all expression stages and functional areas can be detected in immunocompetent HCMV carriers. The fact that memory T cells specific for a significant proportion of these ligands are present in HCMV-seropositive individuals clearly indicates priming of naive T cells against these antigens at any time during infection.

By now, the initial perception that HCMV-specific T cell responses are directed only against a few immunodominant antigens has been challenged by several groups. Using predictive bioinformatics and functional T cell assays, Elington et al. (2003) identified numerous novel HCMV epitopes from a heterogeneous group of 14 preselected proteins (pp28 [UL99], pp50 [UL112-UL113], pp65 [UL83], pp150 [UL32], pp71 [UL82], gH [UL75], gB [UL55], IE1 [UL123], US2, US3, US6, US11, UL16, and UL18) as T cell targets. Sylwester et al. (2005) analyzed overlapping 15-mer peptides from 213 HCMV open reading frames (ORFs) by cytokine flow cytometry. Of the tested ORFs, 70% were shown to be immunogenic for CD4<sup>+</sup> and/or CD8<sup>+</sup> T cells. Immunogenicity was influenced only modestly by ORF expression kinetics and function (Sylwester et al., 2005). Interestingly, besides pp65 and IE1, UL48 was the only tested ORF

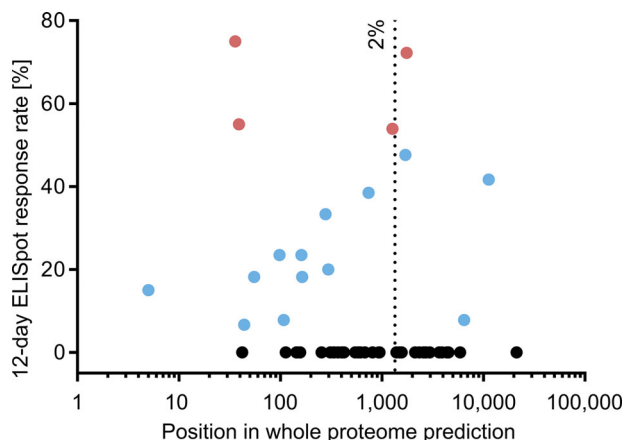


**Figure 5. Position of 9mer ligands assigned to HLA-A\*02:01 in the whole proteome prediction by SYFPEITHI against their immunogenicity.** Dominant and subdominant epitopes are depicted in red and blue, respectively. Nonimmunogenic peptides are depicted in black. The dashed line indicates the best 2% of the prediction that should contain the majority of T cell epitopes according to SYFPEITHI. A possible correlation between the rank of HLA binding affinity predictions and the immunogenicity was assessed with the Kendall rank correlation coefficient tau-b ( $\tau_b = -0.225$ ,  $P = 0.033$ ).



recognized by CD8<sup>+</sup> T cells of >50% of tested donors. In contrast to that particular finding, from a total of 103 identified immunogenic HCMV-derived peptides, 26 epitopes, representing 23 different proteins, were classified as dominant in our study. We found immunogenic peptides from 65 HCMV proteins, confirming previous findings that HCMV-specific CD8<sup>+</sup> T cell immunity in healthy virus carriers is based on a broad repertoire of HCMV antigens. We were able to validate seven previously known epitopes, but some well-established epitopes such as VLEETSVML<sub>IE1/UL123</sub> (A\*02; Khan et al., 2002), YSEHPTFTS-QY<sub>pp65/UL83</sub> (A\*01; Longmate et al., 2001), RPHERNGFTVL<sub>pp65/UL83</sub> (B\*07; Weekes et al., 1999), QIKVRVDMV<sub>IE1/UL123</sub> (B\*08), and ELRRKMMYM<sub>IE1/UL123</sub> (B\*08; Elkington et al., 2003) were not detected in our assays. While our approach has technical limitations, other reasons for the lack of detection of some dominant epitopes are imaginable. The HLA-I antigen presentation pathway could be insufficient for processing of specific peptides in the infected fibroblasts. To assess this, in future studies we will apply IFN $\gamma$  to induce the HLA-I antigen presentation machinery before infection, as IFN $\gamma$  induction strongly improves antigen presentation to CD8<sup>+</sup> T cells (Hengel et al., 1994) and may as well induce HLA-II expression for elution and characterization of class II ligands (Boehm et al., 1997). In addition, ligandome analysis at different time points during infection could yield peptides of different quality. We observed strongly induced numbers of HLA-B\*44:02 ligands in  $\Delta$ US2-6-infected cells, i.e., in the presence of US11 expression. This was indeed surprising, and we have begun to address the molecular mechanisms behind this phenomenon (Zimmermann et al., 2019). Thus, immunoevasins affect not only the efficiency, but also the quality of antigen presentation. Therefore, it should be taken into account that expression of one or combinations of several immunoevasins could result in different HLA-I ligandome qualities. Finally, it cannot be excluded that the  $\Delta$ US2-11 deletion mutant virus still expresses factors that interfere with HLA-I peptide loading and presentation.

The broad CD8<sup>+</sup> T cell response against HCMV detected in healthy donors clearly shows that inhibition of HLA-I antigen presentation by immunoevasins is not sufficient to prevent the induction of CD8<sup>+</sup> T cells (Manley et al., 2004), emphasizing the role of priming of CD8<sup>+</sup> T cells through cross-presentation (Busche et al., 2013). However, HCMV will have a major impact, not only quantitatively, but also qualitatively, on antigen processing and presentation in the infected cells. This could partly explain why a large portion of HCMV-derived ligands fail to elicit a memory response in seropositive donors. Also, different expression/presentation patterns in different cell types could have an effect on memory responses (Frascaroli et al., 2018; Hengel et al., 2000). Such nonimmunogenic ligands might not be processed and presented during an infection in vivo or are not recognized by naive T cells. Furthermore, donors might lack specific naive T cells, leaving a hole in the T cell repertoire (Calis et al., 2012; Rolland et al., 2007; Wölfl et al., 2008). Despite the large number of nonimmunogenic HLA ligands identified, all these peptides are naturally presented on HLA molecules, providing a solid foundation for epitope screening. By using in silico analyses only, it would have been necessary to screen several

thousands of peptides to identify our set of epitopes, as opposed to 368 in our approach.

Infection of various cell cultures expressing distinct HLA allotypes with different HCMV deletion mutants will allow for deeper and broader insights into the quality of viral CD8<sup>+</sup> T cell targets. Moreover, methods such as ribosome profiling will enable the identification of novel ORFs that might be a source of additional viral T cell epitopes (Erhard et al., 2018; Stern-Ginossar et al., 2012). The presence of a broad range of specific memory T cells in healthy seropositive individuals suggests that strategies using subdominant epitopes and targeting multiple antigens in vaccination and cellular therapies may be beneficial for sustainable virus control (Holst et al., 2015; Panagioti et al., 2018; Steffensen et al., 2016). Therefore, the identification of a large number of immunogenic HCMV-derived cytotoxic T cell targets for the most frequent HLA restrictions is, in our opinion, indispensable for the development and improvement of such therapies.

## Materials and methods

### Cells and viruses

MRC-5 fibroblasts (ECACC 05090501) and human foreskin fibroblasts (HF-99/7; kind gift of Dieter Neumann-Haefelin and Valeria Kapper-Falcone, Institute of Virology, Medical Center University of Freiburg, Freiburg, Germany) were grown in DMEM supplemented with 10% FCS, penicillin, and streptomycin.

The AD169VarL-based bacterial artificial chromosome (BAC; Le et al., 2011) mutants were propagated on MRC-5 cells. The HCMV deletion mutants  $\Delta$ US2-6,  $\Delta$ US2-6/ $\Delta$ US11, and  $\Delta$ US2-11 were generated according to a previously published procedure (Wagner et al., 2002) using the BAC-cloned AD169varL genome pAD169 (Le et al., 2011) as parental BAC. Briefly, a PCR fragment was generated using the primers KL-DeltaUS11-Kana1 5'-CAA AAAGTCTGGTGAGTCGTTTCCGAGCGACTCGAGATGCACTCC GCTTCAGTCTATATACCAGTGAATTCGAGCTCGGTAC-3' and KL-DeltaUS11-Kana2 5'-TAAGACAGCCTTACAGCTTTTGAGTCT AGACAGGGTAACAGCCTTCCCTTGTAAGACAGAGACCATGAT TACGCCAAGCTCC-3' and the plasmid pSLFRTKn (Atalay et al., 2002) as template DNA. The PCR fragment containing a kanamycin resistance gene was inserted into the parental BAC by homologous recombination in *Escherichia coli*. Correct mutagenesis was confirmed by Southern blot and PCR analysis. Recombinant HCMVs were reconstituted from HCMV BAC DNA by Superfect (Qiagen; 301305) transfection into permissive MRC-5 cells. Virus titers were determined by standard plaque assay.

### Flow cytometry analysis of infected cells

Cells were detached with Accutase (Sigma-Aldrich; A6964) and stained with antibodies diluted in 3% FCS/PBS. Cells were washed in 3% FCS/PBS supplemented with DAPI and fixed in 3% paraformaldehyde. For intracellular staining of viral Fc receptors, cells were fixed and permeabilized using the BD Cytofix/Cytoperm Kit and stained with Fc-FITC (Rockland Immunochemicals). Cells were measured with a BD FACSCanto II system (BD Biosciences), and acquired data were analyzed by FlowJo (v10.1, TreeStar).

### Analysis of HLA ligands by LC-MS/MS

Approximately  $2-3 \times 10^8$  cells (30 T175 flasks) of MRC-5 fibroblasts (A\*02:01, A\*29:02, B\*07:02, B\*44:02, C\*05:01, and C\*07:02) or human foreskin fibroblasts (HF-99/7; A\*01:01, A\*03:01, B\*08:01, B\*51:01, C\*01:02, and C\*07:01) were infected at an MOI of 4–7. At 48 h.p.i., the cells were collected by scraping and washed three times with PBS. Cell pellets were stored at  $-80^\circ\text{C}$ . HLA-I ligands were isolated using standard immunoaffinity purification using the pan-HLA-I-specific monoclonal antibody W6/32 (Nelde et al., 2019). In brief, cell pellets were thawed and lysed in 10 mM 3-[(3-cholamidopropyl)dimethylammonio]-1-propanesulfonate/PBS (AppliChem/Thermo Fisher Scientific) containing Complete Protease Inhibitor (Roche). The lysate was homogenized by applying pulsed sonification. HLA-I molecules were isolated from the filtered lysate by affinity chromatography with W6/32 antibodies coupled to cyanogen bromide-activated sepharose (GE Healthcare). Repeated addition of 0.2% TFA allowed the elution of HLA/peptide complexes, and subsequent ultrafiltration of the eluate with 3-kD Amicon filter units (Merck Millipore) separated the HLA ligands from the  $\alpha$ - and  $\beta$ -chains of the HLA molecules. After extracting and desalting the ligands from the filtrate using ZipTip C18 pipette tips (Merck Millipore) and 0.1% TFA, elution was performed with 32% acetonitrile (AcN)/0.2% TFA. The elution solution was reduced in a vacuum centrifuge and filled with 1% AcN/0.2% TFA. HLA ligand extracts were analyzed as described previously (Nelde et al., 2019). In brief, HLA ligand extracts were separated by reversed-phase LC (nanoUHPLC, UltiMate 3000RSLCnano; Dionex) using a  $75 \mu\text{m} \times 25 \text{ cm}$  PepMap C18 column (Thermo Fisher Scientific). Linear gradients were applied ranging from 2.4% to 32% AcN over the course of 90 min in almost all analyses. In single experiments, other methods were tested, applying 195- or 300-min gradients on a  $75 \mu\text{m} \times 50 \text{ cm}$  PepMap column. Peptides eluted from MRC-5 cells were analyzed in an online coupled LTQ Orbitrap XL mass spectrometer (Thermo Fisher Scientific) using a top-five collision-induced dissociation method generating ion trap MS/MS spectra. Extracts of HF-99/7 cells were analyzed in an online coupled LTQ Orbitrap Fusion Lumos mass spectrometer (Thermo Fisher Scientific) using a top-speed collision-induced dissociation method leading to Orbitrap MS/MS spectra.

### Database search and filtering

Data processing was performed as described previously (Kowalewski et al., 2015). In brief, the Mascot search engine (Mascot 2.2.04; Matrix Science, for ion trap fragment spectra) or the SEQUEST HT search engine (University of Washington, for Orbitrap fragment spectra; Eng et al., 1994) were used to search the human and HCMV proteome. Fragment spectra were searched against a concatenated FASTA consisting of the reviewed Swiss-Prot human (March 2014; 20,271 sequences) and HCMV (March 2014; 400 sequences) proteomes. The search combined data of technical replicates and was not restricted by enzymatic specificity. Precursor mass tolerance was set to 5 ppm, and fragment mass tolerance was set to 0.5 daltons for ion trap spectra analyzed by Mascot and 0.02 daltons for Orbitrap spectra analyzed by SEQUEST HT. Oxidized methionine was

allowed as dynamic modification. FDR was estimated using the Percolator algorithm (Käll et al., 2007). Identifications were filtered to an FDR of 5% assessed on peptide spectrum match level, search engine rank = 1, and peptide lengths of 8–12 aa. For Mascot database searches, the additional filter of Mascot Ion Scores  $\geq 20$  was used. All peptide identifications were annotated to their respective HLA motifs using both SYFPEITHI (Rammensee et al., 1999) and NetMHC (Lundegaard et al., 2008). The MRC-5 dataset was annotated with NetMHC (version 3.4; Lundegaard et al., 2008), and the HF-99/7 dataset with NetMHCpan (version 3.0; Nielsen and Andreatta, 2016). A normalized SYFPEITHI score of  $\geq 50\%$  and NetMHC  $\text{IC}_{50} \leq 500 \text{ nM}$  as well as a percentile rank  $< 2\%$  for NetMHCpan3.0 were applied as cutoffs. The normalized SYFPEITHI score indicates the percentage of the possible maximum score for the respective HLA allele and length of the scored peptide. Peptides fulfilling the cutoff in either or both prediction tools were designated predicted HLA ligands in this article. In case of multiple possible annotations, the HLA allotype yielding the best rank/score was selected. Peptides were tested in donor samples of different restrictions if the two algorithms resulted in inconsistent allotype annotations.

### Peptide and HLA:peptide monomer synthesis

Synthetic peptides were produced by standard 9-fluorenylmethyloxycarbonyl/tert-butyl strategy using peptide synthesizers 433A (Applied Biosystems), P11 (Activotec) or Liberty Blue (CEM). Purity was assessed by reversed-phase HPLC (e2695, Waters) and identity affirmed by nano-UHPLC (UltiMate 3000 RSLCnano) coupled online to a hybrid mass spectrometer (LTQ Orbitrap XL, both Thermo Fisher Scientific). Lyophilized peptides were dissolved at 10 mg/ml in DMSO and diluted 1:10 in bidistilled  $\text{H}_2\text{O}$ . Frozen aliquots were further diluted in cell culture medium and sterile filtered if necessary. Synthetic peptides were used for validation of LC-MS/MS identifications as well as for functional experiments. Biotinylated recombinant HLA molecules and fluorescent HLA:peptide tetramers were produced as described previously (Garboczi et al., 1992; Peper et al., 2015; Rodenko et al., 2006).

### Target cell infection for cytotoxicity assays

MRC-5 cells were cultured in DMEM (1 $\times$ ; Thermo Fisher Scientific; 41965039) supplemented with 10% FCS, 100 U/ml penicillin, and 100  $\mu\text{g}/\text{ml}$  streptomycin at  $37^\circ\text{C}$  and 7.5%  $\text{CO}_2$ . For cytotoxicity assays, MRC-5 cells were infected with varying MOI and subsequently centrifuged for 30 min at 300  $g$ . After resting for  $\sim 1 \text{ h}$ , cells were harvested by trypsinization for 2 min at  $37^\circ\text{C}$  and seeded in E-plates 96 (ACEA Biosciences; 05232368001) with 20,000 cells per well.

### T cell culture

Buffy coats were kindly provided by the Institute for Clinical and Experimental Transfusion Medicine at the University Hospital of Tübingen after obtaining written informed consent in accordance with the Declaration of Helsinki and applicable laws and regulations. This has been approved by the Ethik-Kommission an der Medizinischen Fakultät der Eberhard-Karls-Universität und

am Universitätsklinikum Tübingen (Project No. 507/2017BO1). Two-digit HLA-A and -B typing and CMV status were provided by Transfusion Medicine. Thereafter, blood samples were encoded by four-digit numbers. Peripheral blood mononuclear cells (PBMCs) were isolated from healthy HCMV-seropositive blood donors by Ficoll-Hypaque density gradient centrifugation. Cells were frozen at  $-80^{\circ}\text{C}$  in FCS and 10% DMSO. After thawing, cells were rested overnight before stimulation. Culture conditions were 7.5%  $\text{CO}_2$  and  $37^{\circ}\text{C}$  in humidified incubators in IMDM (Thermo Fisher Scientific; 12440) supplemented with 5% heat-inactivated pooled human plasma (isolated from healthy blood donors), 100 U/ml penicillin, 100  $\mu\text{g}/\text{ml}$  streptomycin, 25  $\mu\text{g}/\text{ml}$  gentamicin (Life Technologies), and 50  $\mu\text{M}$   $\beta$ -mercaptoethanol (Carl Roth).

### IFN $\gamma$ ELISpot assay

IFN $\gamma$  ELISpot assays were performed after 12-d stimulation as described previously (Peper et al., 2015) or directly ex vivo 1 d after thawing. For the 12-d stimulation, PBMCs were stimulated 1 d after thawing (day 1) with a pool of  $\leq 10$  peptides of interest and the negative control peptide. Each peptide had a final concentration of 1  $\mu\text{g}/\text{ml}$ . IL-2 was added on days 2, 5, and 7 with a final concentration of 20 U/ml. On day 12, cells were harvested, and 500,000 cells per well were seeded onto nitrocellulose plates (Merck Millipore). The cells were then incubated for 24 h together with 1  $\mu\text{g}/\text{ml}$  of a peptide of interest, the negative control, or PHA. Readout was performed according to the manufacturer's recommendation and the cancer immunotherapy monitoring panel (Britten et al., 2008). PHA was used as a positive control. The following peptides, served as negative controls: GSEELRSly HIV POL<sub>71-79</sub> (A\*01), YLLPAIVHI HUMAN DDX5<sub>148-156</sub> (A\*02), RLRPGGKKK HIV GAG<sub>20-28</sub> (A\*03), TPGPGVRYPL, HIV Nef<sub>128-137</sub> (B\*07), GGKKKYKL HIV GAG<sub>24-31</sub> (B\*08), EEIPASDDVLF HCMV DNBI<sub>1095-1105</sub> (B\*44), and DPY-KATSAV HUMAN MUC16<sub>6326-6334</sub> (B\*51). DMSO was used as a negative control for HLA-A\*29. Blue spots specific for IFN $\gamma$ -producing cells were automatically counted using an ImmunoSpot S5 analyzer (CTL) and ImmunoSpot software. T cell responses were considered to be positive when  $>10$  spots/well were counted and the mean spot count per well was at least threefold higher than the mean number of spots in negative control wells. Background staining due to excess cytokine and overlapping spots hamper the detection of reliable counts in wells of highly responsive donors. Therefore, spot counts of  $>1,000$  or "too numerous to count" were set to 1,000.

### Analysis of T cells

HLA tetramer staining of T cells was performed by incubation with 5  $\mu\text{g}/\text{ml}$  tetramer diluted in tetramer staining buffer (2% FCS, 0.01% sodium azide, and 2 mM EDTA in PBS) for 30 min at  $4^{\circ}\text{C}$ . Afterwards, T cells were stained with CD8-PerCP (BioLegend; 301030) for 20 min at  $4^{\circ}\text{C}$ .

For ICS, 0.5–1 Mio cells/well were stimulated with individual peptides (10  $\mu\text{g}/\text{ml}$ ) in the presence of brefeldin A (Sigma-Aldrich; B7651), GolgiStop (BD Biosciences; 554724) and anti-CD107a-FITC monoclonal antibody (BD Biosciences; 555800) at 150  $\mu\text{l}$  per well for 12–14 h. After incubation, cells were washed

and stained with anti-CD8-PerCP (BioLegend; 301030) and anti-CD4-APC (BioLegend; 300518) antibodies followed by fixation and permeabilization for a further 20 min at  $4^{\circ}\text{C}$  (Cytofix/Cytoperm; BD Biosciences). After washing with permwash buffer, cytokines were stained with anti-TNF-PacificBlue (BioLegend; 502920) and anti-IFN $\gamma$ -PE (BioLegend; 506507) antibodies for 20 min at  $4^{\circ}\text{C}$ . Flow cytometric measurements were performed on a FACSCanto II cytometer (BD Biosciences) and analyzed using FlowJo version 10.

### T cell clones

PBMCs of HLA-matched seropositive donors were stimulated with 1  $\mu\text{g}/\text{ml}$  specific peptide 1 d after thawing and with IL-2 (20 U/ml; R&D Systems; 202-IL) on days 2 and 5. On day 14, HLA tetramer staining was performed, and tetramer-positive CD8 $^{+}$  T cells were sorted in 96-well plates containing  $1.5 \times 10^5$  irradiated PBMCs (60-Gray, 1000 Elite Gammacell),  $1.5 \times 10^4$  irradiated LG2-EBV (200 Gray; kind gift from Pierre van der Bruggen, Ludwig Institute for Cancer Research, Brussels, Belgium) as feeder cells, 150 U/ml IL-2, and 0.5  $\mu\text{g}/\text{ml}$  PHA-L (Sigma-Aldrich; 11249738001) in 150  $\mu\text{l}$  medium per well. Sorting was performed using BD FACSJazz equipped with BD FACS software. Five or 10 tetramer-positive CD8 $^{+}$  T cells were sorted per well and incubated at  $37^{\circ}\text{C}$  and 7.5%  $\text{CO}_2$ . After resting for 1 wk, cells were stimulated twice per week with 150 U/ml IL-2, and freshly irradiated feeder cells were added every second or third week together with 150 U/ml IL-2 and 1  $\mu\text{g}/\text{ml}$  PHA-L.

### Real-time cytotoxicity assay (xCELLigence)

Real-time cytotoxicity assays were performed as described previously (Peper et al., 2014). All experiments were performed in DMEM with 10% FCS and 1% penicillin/streptomycin. Background values were determined using 50  $\mu\text{l}$  medium per well. MRC-5 cells, infected or mock-treated, were seeded in 96-well E-plates (ACEA Biosciences; 05232368001) at a concentration of 20,000 cells per well in 50  $\mu\text{l}$  medium. Effector cells were added 48 h after target cells in indicated E:T cell ratios. For peptide loading of MRC-5 cells, synthetic peptides (final concentration 1  $\mu\text{g}/\text{ml}$ ) were added to target cells 1 h before effector cells. Cell attachment was monitored using the RTCA SP (Roche) instrument and RTCA software version 1.1 (Roche). Impedance measurements were performed every 15 min for up to 140 h. All experiments were performed in triplicates.

### Whole proteome prediction

SYFPEITHI and NetMHCpan3.0 were employed for the in silico epitope prediction (Schubert et al., 2016) of the whole HCMV proteome using a concatenated FASTA consisting of the reviewed Swiss-Prot HCMV AD169 proteome (March 2014; 193 sequences) and the reviewed sequences of UL133, UL135, UL136, UL138-UL142, UL144-UL148, UL150, and UL147A of strain Merlin (Le et al., 2011). The additional proteins are part of the ULb' region that is included in the BAC construct used.

### Statistical analysis

The correspondence of the proteome-wide rank of the SYFPEITHI HLA binding affinity predictions and the experimentally



determined immunogenicity was assessed by calculating the Kendall rank correlation coefficient ( $\tau_b$ ) and its respective P value using the `cor.test` function as part of the stats package in the R statistical computing environment (v3.5; R Core Team, 2018).

#### Data availability

The MS data have been deposited to the ProteomeXchange Consortium via the PRIDE (Perez-Riverol et al., 2019) partner repository with the dataset identifier PXD013120.

#### Online supplemental material

Fig. S1 shows the determination of the infection rate of the analyzed cells before ligand extraction. Fig. S2 shows an overlap analysis of the HCMV-derived ligands extracted from five independent infections of MRC-5 cells with  $\Delta$ US2-6/ $\Delta$ US11. Fig. S3 depicts the ELISpot results for each epitope. Fig. S4 shows the parallel recognition of multiple epitopes by PBMC donors. Fig. S5 contains further information about the tests before the cytotoxicity assays. Table S1 lists all identified T cell epitopes and the results of ELISpot assays, ICS, and tetramer stainings. Table S2 shows the position of dominant epitopes within the whole proteome prediction with NetMHCpan3.0 and SYFPEITHI. Dataset S1 lists all ligands identified from extracts of MRC-5 cells. Dataset S2 contains the comparison of annotated fragment spectra of 50 randomly selected HCMV-derived HLA ligand identifications with their synthetic counterparts. Spectral pairs found to be mismatching in manual evaluation based on missing fragment ions in the natural spectrum or mismatching intensity distributions are outlined in red. Dataset S3 lists all HLA ligands identified from extracts of HF-99/7 cells.

#### Acknowledgments

This work was supported by the German Ministry of Education and Research as part of the German Network for Bioinformatics infrastructure (FKZ: 31A535A) and the Deutsche Forschungsgemeinschaft as part of the Research Unit "Advanced Concepts in Cellular Immune Control of Cytomegalovirus" (FOR2830).

Author contributions: H. Hengel, H.-G. Rammensee, S. Stevanović, and A. Halenius designed the study. D.J. Kowalewski, A. Nelde, and A. Marcu performed HLA ligandome experiments. M. Lübke, S. Spalt, and J.K. Peper performed in vitro T cell experiments. V.T.K. Le-Trilling and A. Halenius designed and provided deletion viruses. Infection experiments were conducted by C. Zimmermann and L. Bauersfeld. L. Bichmann performed the whole proteome prediction and statistical analysis. S. Spalt, D.J. Kowalewski, C. Zimmermann, A. Nelde, A. Marcu, and J.S. Walz analyzed data. M. Lübke, S. Spalt, D.J. Kowalewski, and A. Halenius wrote the manuscript in consultation with O. Kohlbacher, H. Hengel, H.-G. Rammensee, and S. Stevanović. H.-G. Rammensee, S. Stevanović, and A. Halenius supervised the project.

Disclosures: M. Lübke reported a patent to HCMV epitopes (pending). S. Spalt reported a patent to HCMV epitopes

(pending) and is currently an employee of Immatics Biotechnologies GmbH. D.J. Kowalewski reported a patent to HCMV epitopes (pending) and is currently an employee of Immatics Biotechnologies. C. Zimmermann reported a patent to HCMV epitopes (pending). L. Bauersfeld reported a patent to HCMV epitopes (pending). A. Nelde reported a patent to HCMV epitopes (pending). V.T.K. Le-Trilling reported a patent to HCMV epitopes (pending). H. Hengel reported a patent to HCMV epitopes (pending). H.-G. Rammensee reported "other" from Immatics GmbH and "other" from Curevac AG during the conduct of the study; in addition, H.-G. Rammensee had a patent to HCMV epitopes (pending). A. Halenius reported a patent to HCMV epitopes (pending). No other disclosures were reported.

Submitted: 25 June 2019

Revised: 24 October 2019

Accepted: 12 November 2019

#### References

- Ahn, K., A. Gruhler, B. Galocha, T.R. Jones, E.J. Wiertz, H.L. Ploegh, P.A. Peterson, Y. Yang, and K. Früh. 1997. The ER-luminal domain of the HCMV glycoprotein US6 inhibits peptide translocation by TAP. *Immunity*. 6:613–621. [https://doi.org/10.1016/S1074-7613\(00\)80349-0](https://doi.org/10.1016/S1074-7613(00)80349-0)
- Akiyama, Y., K. Maruyama, T. Mochizuki, K. Sasaki, Y. Takaue, and K. Yamaguchi. 2002. Identification of HLA-A24-restricted CTL epitope encoded by the matrix protein pp65 of human cytomegalovirus. *Immunol. Lett.* 83:21–30. [https://doi.org/10.1016/S0165-2478\(02\)00073-1](https://doi.org/10.1016/S0165-2478(02)00073-1)
- Atalay, R., A. Zimmermann, M. Wagner, E. Borst, C. Benz, M. Messerle, and H. Hengel. 2002. Identification and expression of human cytomegalovirus transcription units coding for two distinct Fcγ receptor homologs. *J. Virol.* 76:8596–8608. <https://doi.org/10.1128/JVI.76.17.8596-8608.2002>
- Boehm, U., T. Klamp, M. Groot, and J.C. Howard. 1997. Cellular responses to interferon-gamma. *Annu. Rev. Immunol.* 15:749–795. <https://doi.org/10.1146/annurev.immunol.15.1.749>
- Britten, C.M., C. Gouttefangeas, M.J. Welters, G. Pawelec, S. Koch, C. Ottensmeier, A. Mander, S. Walter, A. Paschen, J. Müller-Berghaus, et al. 2008. The CIMT-monitoring panel: a two-step approach to harmonize the enumeration of antigen-specific CD8+ T lymphocytes by structural and functional assays. *Cancer Immunol. Immunother.* 57:289–302. <https://doi.org/10.1007/s00262-007-0378-0>
- Busche, A., A.C. Jirno, S.P. Welten, J. Zischke, J. Noack, H. Constabel, A.K. Gatzke, K.A. Keyser, R. Arens, G.M. Behrens, and M. Messerle. 2013. Priming of CD8+ T cells against cytomegalovirus-encoded antigens is dominated by cross-presentation. *J. Immunol.* 190:2767–2777. <https://doi.org/10.4049/jimmunol.1200966>
- Calis, J.J., R.J. de Boer, and C. Keşmir. 2012. Degenerate T-cell recognition of peptides on MHC molecules creates large holes in the T-cell repertoire. *PLOS Comput. Biol.* 8:e1002412. <https://doi.org/10.1371/journal.pcbi.1002412>
- Croft, N.P., S.A. Smith, J. Pickering, J. Sidney, B. Peters, P. Faridi, M.J. Witney, P. Sebastian, I.E.A. Flesch, S.L. Heading, et al. 2019. Most viral peptides displayed by class I MHC on infected cells are immunogenic. *Proc. Natl. Acad. Sci. USA*. 116:3112–3117. <https://doi.org/10.1073/pnas.1815239116>
- Einsele, H., E. Roosnek, N. Rufer, C. Sinzger, S. Riegler, J. Löffler, U. Grigoleit, A. Moris, H.G. Rammensee, L. Kanz, et al. 2002. Infusion of cytomegalovirus (CMV)-specific T cells for the treatment of CMV infection not responding to antiviral chemotherapy. *Blood*. 99:3916–3922. <https://doi.org/10.1182/blood.V99.11.3916>
- Elkington, R., S. Walker, T. Crough, M. Menzies, J. Tellam, M. Bharadwaj, and R. Khanna. 2003. Ex vivo profiling of CD8+ T-cell responses to human cytomegalovirus reveals broad and multispecific reactivities in healthy virus carriers. *J. Virol.* 77:5226–5240. <https://doi.org/10.1128/JVI.77.9.5226-5240.2003>
- Eng, J.K., A.L. McCormack, and J.R. Yates. 1994. An approach to correlate tandem mass spectral data of peptides with amino acid sequences in a protein database. *J. Am. Soc. Mass Spectrom.* 5:976–989. [https://doi.org/10.1016/1044-0305\(94\)80016-2](https://doi.org/10.1016/1044-0305(94)80016-2)



- Erhard, F., A. Halenius, C. Zimmermann, A. L'Hernault, D.J. Kowalewski, M.P. Weekes, S. Stevanovic, R. Zimmer, and L. Dölken. 2018. Improved Ribo-seq enables identification of cryptic translation events. *Nat. Methods*. 15:363–366. <https://doi.org/10.1038/nmeth.4631>
- Frascaroli, G., C. Lecher, S. Varani, C. Setz, J. van der Merwe, W. Brune, and T. Mertens. 2018. Human Macrophages Escape Inhibition of Major Histocompatibility Complex-Dependent Antigen Presentation by Cytomegalovirus and Drive Proliferation and Activation of Memory CD4<sup>+</sup> and CD8<sup>+</sup> T Cells. *Front. Immunol.* 9:1129. <https://doi.org/10.3389/fimmu.2018.01129>
- Fülöp, T., A. Larbi, and G. Pawelec. 2013. Human T cell aging and the impact of persistent viral infections. *Front. Immunol.* 4:271. <https://doi.org/10.3389/fimmu.2013.00271>
- Furman, M.H., N. Dey, D. Tortorella, and H.L. Ploegh. 2002. The human cytomegalovirus US10 gene product delays trafficking of major histocompatibility complex class I molecules. *J. Virol.* 76:11753–11756. <https://doi.org/10.1128/JVI.76.22.11753-11756.2002>
- Garboczi, D.N., D.T. Hung, and D.C. Wiley. 1992. HLA-A2-peptide complexes: refolding and crystallization of molecules expressed in *Escherichia coli* and complexed with single antigenic peptides. *Proc. Natl. Acad. Sci. USA*. 89:3429–3433. <https://doi.org/10.1073/pnas.89.8.3429>
- Gewurz, B.E., R. Gaudet, D. Tortorella, E.W. Wang, H.L. Ploegh, and D.C. Wiley. 2001. Antigen presentation subverted: Structure of the human cytomegalovirus protein US2 bound to the class I molecule HLA-A2. *Proc. Natl. Acad. Sci. USA*. 98:6794–6799. <https://doi.org/10.1073/pnas.121172898>
- Günther, P.S., J.K. Peper, B. Faist, S. Kayser, L. Hartl, T. Feuchtinger, G. Jahn, M. Neuenhahn, D.H. Busch, S. Stevanović, and K.M. Denhehy. 2015. Identification of a Novel Immunodominant HLA-B\*07: 02-restricted Adenoviral Peptide Epitope and Its Potential in Adoptive Transfer Immunotherapy. *J. Immunother.* 38:267–275. <https://doi.org/10.1097/CJI.0000000000000087>
- Harkins, L., A.L. Volk, M. Samanta, I. Mikolaenko, W.J. Britt, K.I. Bland, and C.S. Cobbs. 2002. Specific localisation of human cytomegalovirus nucleic acids and proteins in human colorectal cancer. *Lancet*. 360: 1557–1563. [https://doi.org/10.1016/S0140-6736\(02\)11524-8](https://doi.org/10.1016/S0140-6736(02)11524-8)
- Hebart, H., S. Deginik, S. Stevanovic, U. Grigoleit, A. Dobler, M. Baur, G. Rauser, C. Sinzger, G. Jahn, J. Loeffler, et al. 2002. Sensitive detection of human cytomegalovirus peptide-specific cytotoxic T-lymphocyte responses by interferon-gamma-enzyme-linked immunospot assay and flow cytometry in healthy individuals and in patients after allogeneic stem cell transplantation. *Blood*. 99:3830–3837. <https://doi.org/10.1182/blood.V99.10.3830>
- Hegde, N.R., R.A. Tomazin, T.W. Wisner, C. Dunn, J.M. Boname, D.M. Lewinsohn, and D.C. Johnson. 2002. Inhibition of HLA-DR assembly, transport, and loading by human cytomegalovirus glycoprotein US3: a novel mechanism for evading major histocompatibility complex class II antigen presentation. *J. Virol.* 76:10929–10941. <https://doi.org/10.1128/JVI.76.21.10929-10941.2002>
- Hengel, H., P. Lucin, S. Jonjić, T. Ruppert, and U.H. Koszinowski. 1994. Restoration of cytomegalovirus antigen presentation by gamma interferon combats viral escape. *J. Virol.* 68:289–297.
- Hengel, H., U. Reusch, G. Geginat, R. Holtappels, T. Ruppert, E. Hellebrand, and U.H. Koszinowski. 2000. Macrophages escape inhibition of major histocompatibility complex class I-dependent antigen presentation by cytomegalovirus. *J. Virol.* 74:7861–7868. <https://doi.org/10.1128/JVI.74.17.7861-7868.2000>
- Hewitt, E.W., S.S. Gupta, and P.J. Lehner. 2001. The human cytomegalovirus gene product US6 inhibits ATP binding by TAP. *EMBO J.* 20:387–396. <https://doi.org/10.1093/emboj/20.3.387>
- Holst, P.J., B.A. Jensen, E. Ragonnaud, A.R. Thomsen, and J.P. Christensen. 2015. Targeting of non-dominant antigens as a vaccine strategy to broaden T-cell responses during chronic viral infection. *PLoS One*. 10: e0117242. <https://doi.org/10.1371/journal.pone.0117242>
- Jones, T.R., and L. Sun. 1997. Human cytomegalovirus US2 destabilizes major histocompatibility complex class I heavy chains. *J. Virol.* 71:2970–2979.
- Jones, T.R., E.J. Wiertz, L. Sun, K.N. Fish, J.A. Nelson, and H.L. Ploegh. 1996. Human cytomegalovirus US3 impairs transport and maturation of major histocompatibility complex class I heavy chains. *Proc. Natl. Acad. Sci. USA*. 93:11327–11333. <https://doi.org/10.1073/pnas.93.21.11327>
- Käll, L., J.D. Canterbury, J. Weston, W.S. Noble, and M.J. MacCoss. 2007. Semi-supervised learning for peptide identification from shotgun proteomics datasets. *Nat. Methods*. 4:923–925. <https://doi.org/10.1038/nmeth1113>
- Kern, F., I.P. Sural, N. Faulhaber, C. Frömmel, J. Schneider-Mergener, C. Schönemann, P. Reinke, and H.D. Volk. 1999. Target structures of the CD8(+) T-cell response to human cytomegalovirus: the 72-kilodalton major immediate-early protein revisited. *J. Virol.* 73:8179–8184.
- Khan, N., M. Cobbold, R. Keenan, and P.A. Moss. 2002. Comparative analysis of CD8<sup>+</sup> T cell responses against human cytomegalovirus proteins pp65 and immediate early 1 shows similarities in precursor frequency, oligoclonality, and phenotype. *J. Infect. Dis.* 185:1025–1034. <https://doi.org/10.1086/339963>
- Kowalewski, D.J., H. Schuster, L. Backert, C. Berlin, S. Kahn, L. Kanz, H.R. Salih, H.G. Rammensee, S. Stevanovic, and J.S. Stickel. 2015. HLA ligandome analysis identifies the underlying specificities of spontaneous antileukemia immune responses in chronic lymphocytic leukemia (CLL). *Proc. Natl. Acad. Sci. USA*. 112:E166–E175. <https://doi.org/10.1073/pnas.1416389112>
- Le, V.T., M. Trilling, and H. Hengel. 2011. The cytomegaloviral protein pUL138 acts as potentiator of tumor necrosis factor (TNF) receptor 1 surface density to enhance ULB'-encoded modulation of TNF- $\alpha$  signaling. *J. Virol.* 85:13260–13270. <https://doi.org/10.1128/JVI.06005-11>
- Le Roy, E., and J.L. Davignon. 2005. Human cytomegalovirus-specific CD4(+) T-cell clones recognize cross-reactive peptides from the immediate early 1 protein. *Viral Immunol.* 18:391–396. <https://doi.org/10.1089/vim.2005.18.391>
- Li, S., J. Zhu, W. Zhang, Y. Chen, K. Zhang, L.M. Popescu, X. Ma, W.B. Lau, R. Rong, X. Yu, et al. 2011. Signature microRNA expression profile of essential hypertension and its novel link to human cytomegalovirus infection. *Circulation*. 124:175–184. <https://doi.org/10.1161/CIRCULATIONAHA.110.012237>
- Longmate, J., J. York, C. La Rosa, R. Krishnan, M. Zhang, D. Senitzer, and D.J. Diamond. 2001. Population coverage by HLA class-I restricted cytotoxic T-lymphocyte epitopes. *Immunogenetics*. 52:165–173. <https://doi.org/10.1007/s002510000271>
- Lundegaard, C., O. Lund, and M. Nielsen. 2008. Accurate approximation method for prediction of class I MHC affinities for peptides of length 8, 10 and 11 using prediction tools trained on 9mers. *Bioinformatics*. 24: 1397–1398. <https://doi.org/10.1093/bioinformatics/btn128>
- Manley, T.J., L. Luy, T. Jones, M. Boeckh, H. Mutimer, and S.R. Riddell. 2004. Immune evasion proteins of human cytomegalovirus do not prevent a diverse CD8<sup>+</sup> cytotoxic T-cell response in natural infection. *Blood*. 104: 1075–1082. <https://doi.org/10.1182/blood-2003-06-1937>
- McLaughlin-Taylor, E., H. Pande, S.J. Forman, B. Tanamachi, C.R. Li, J.A. Zaia, P.D. Greenberg, and S.R. Riddell. 1994. Identification of the major late human cytomegalovirus matrix protein pp65 as a target antigen for CD8<sup>+</sup> virus-specific cytotoxic T lymphocytes. *J. Med. Virol.* 43:103–110. <https://doi.org/10.1002/jmv.1890430119>
- McMurtrey, C.P., A. Lelic, P. Piazza, A.K. Chakrabarti, E.J. Yablonsky, A. Wahl, W. Bardet, A. Eckerd, R.L. Cook, R. Hess, et al. 2008. Epitope discovery in West Nile virus infection: Identification and immune recognition of viral epitopes. *Proc. Natl. Acad. Sci. USA*. 105:2981–2986. <https://doi.org/10.1073/pnas.0711874105>
- Meyer, V.S., W. Kastenmuller, G. Gasteiger, M. Franz-Wachtel, T. Lamkemeyer, H.G. Rammensee, S. Stevanovic, D. Sigurdardottir, and I. Drexler. 2008. Long-term immunity against adult poxviral HLA ligands as identified by differential stable isotope labeling. *J. Immunol.* 181:6371–6383. <https://doi.org/10.4049/jimmunol.181.9.6371>
- Nastke, M.D., L. Herrgen, S. Walter, D. Wernet, H.G. Rammensee, and S. Stevanović. 2005. Major contribution of codominant CD8 and CD4 T cell epitopes to the human cytomegalovirus-specific T cell repertoire. *Cell. Mol. Life Sci.* 62:77–86. <https://doi.org/10.1007/s00018-004-4363-x>
- Nelke, A., D.J. Kowalewski, and S. Stevanović. 2019. Purification and Identification of Naturally Presented MHC Class I and II Ligands. *Methods Mol. Biol.* 1988:123–136. [https://doi.org/10.1007/978-1-4939-9450-2\\_10](https://doi.org/10.1007/978-1-4939-9450-2_10)
- Nielsen, M., and M. Andreatta. 2016. NetMHCpan-3.0; improved prediction of binding to MHC class I molecules integrating information from multiple receptor and peptide length datasets. *Genome Med.* 8:33. <https://doi.org/10.1186/s13073-016-0288-x>
- Odeberg, J., B. Plachter, L. Brandén, and C. Söderberg-Nauclér. 2003. Human cytomegalovirus protein pp65 mediates accumulation of HLA-DR in lysosomes and destruction of the HLA-DR alpha-chain. *Blood*. 101: 4870–4877. <https://doi.org/10.1182/blood-2002-05-1504>
- Panagioti, E., P. Klenerman, L.N. Lee, S.H. van der Burg, and R. Arens. 2018. Features of Effective T Cell-Inducing Vaccines against Chronic Viral Infections. *Front. Immunol.* 9:276. <https://doi.org/10.3389/fimmu.2018.00276>
- Peper, J.K., H.C. Bösmüller, H. Schuster, B. Gückel, H. Hörzer, K. Roehle, R. Schäfer, P. Wagner, H.G. Rammensee, S. Stevanović, et al. 2015. HLA ligandomics identifies histone deacetylase 1 as target for ovarian cancer immunotherapy. *OncolImmunology*. 5:e1065369. <https://doi.org/10.1080/2162402X.2015.1065369>

- Peper, J.K., H. Schuster, M.W. Löffler, B. Schmid-Horch, H.G. Rammensee, and S. Stevanović. 2014. An impedance-based cytotoxicity assay for real-time and label-free assessment of T-cell-mediated killing of adherent cells. *J. Immunol. Methods*. 405:192–198. <https://doi.org/10.1016/j.jim.2014.01.012>
- Perez-Riverol, Y., A. Csordas, J. Bai, M. Bernal-Llinares, S. Hewapathirana, D.J. Kundu, A. Inuganti, J. Griss, G. Mayer, M. Eisenacher, et al. 2019. The PRIDE database and related tools and resources in 2019: improving support for quantification data. *Nucleic Acids Res.* 47(D1):D442–D450. <https://doi.org/10.1093/nar/gky1106>
- Plotkin, S.A., and S.B. Boppana. 2018. Vaccination against the human cytomegalovirus. *Vaccine*. doi: 10.1016/j.vaccine.2018.02.089.
- Quinnan, G.V. Jr., N. Kirmani, A.H. Rook, J.F. Manischewitz, L. Jackson, G. Moreschi, G.W. Santos, R. Saral, and W.H. Burns. 1982. Cytotoxic t cells in cytomegalovirus infection: HLA-restricted T-lymphocyte and non-T-lymphocyte cytotoxic responses correlate with recovery from cytomegalovirus infection in bone-marrow-transplant recipients. *N. Engl. J. Med.* 307:7–13. <https://doi.org/10.1056/NEJM198207013070102>
- R Core Team. 2018. R: A Language and Environment for Statistical Computing. R Foundation for Statistical Computing, Vienna, Austria.
- Rammensee, H., J. Bachmann, N.P. Emmerich, O.A. Bachor, and S. Stevanović. 1999. SYFPEITHI: database for MHC ligands and peptide motifs. *Immunogenetics*. 50:213–219. <https://doi.org/10.1007/s002510050595>
- Reusser, P., S.R. Riddell, J.D. Meyers, and P.D. Greenberg. 1991. Cytotoxic T-lymphocyte response to cytomegalovirus after human allogeneic bone marrow transplantation: pattern of recovery and correlation with cytomegalovirus infection and disease. *Blood*. 78:1373–1380. <https://doi.org/10.1182/blood.V78.5.1373.1373>
- Rodenko, B., M. Toebe, S.R. Hadrup, W.J. van Esch, A.M. Molenaar, T.N. Schumacher, and H. Ovaa. 2006. Generation of peptide-MHC class I complexes through UV-mediated ligand exchange. *Nat. Protoc.* 1: 1120–1132. <https://doi.org/10.1038/nprot.2006.121>
- Rolland, M., D.C. Nickle, W. Deng, N. Frahm, C. Brander, G.H. Learn, D. Heckerman, N. Jovic, V. Jovic, B.D. Walker, and J.I. Mullins. 2007. Recognition of HIV-1 peptides by host CTL is related to HIV-1 similarity to human proteins. *PLoS One*. 2:e823. <https://doi.org/10.1371/journal.pone.0000823>
- Schubert, B., M. Walzer, H.P. Brachvogel, A. Szolek, C. Mohr, and O. Kohlbacher. 2016. FRED 2: an immunoinformatics framework for Python. *Bioinformatics*. 32:2044–2046. <https://doi.org/10.1093/bioinformatics/btw113>
- Söderberg-Nauclér, C. 2006. Does cytomegalovirus play a causative role in the development of various inflammatory diseases and cancer? *J. Intern. Med.* 259:219–246. <https://doi.org/10.1111/j.1365-2796.2006.01618.x>
- Söderberg-Nauclér, C. 2008. HCMV microinfections in inflammatory diseases and cancer. *J. Clin. Virol.* 41:218–223. <https://doi.org/10.1016/j.jcv.2007.11.009>
- Staras, S.A., S.C. Dollard, K.W. Radford, W.D. Flanders, R.F. Pass, and M.J. Cannon. 2006. Seroprevalence of cytomegalovirus infection in the United States, 1988–1994. *Clin. Infect. Dis.* 43:1143–1151. <https://doi.org/10.1086/508173>
- Steffensen, M.A., L.H. Pedersen, M.L. Jahn, K.N. Nielsen, J.P. Christensen, and A.R. Thomsen. 2016. Vaccine Targeting of Subdominant CD8+ T Cell Epitopes Increases the Breadth of the T Cell Response upon Viral Challenge, but May Impair Immediate Virus Control. *J. Immunol.* 196: 2666–2676. <https://doi.org/10.4049/jimmunol.1502018>
- Stern-Ginossar, N., B. Weisburd, A. Michalski, V.T. Le, M.Y. Hein, S.X. Huang, M. Ma, B. Shen, S.B. Qian, H. Hengel, et al. 2012. Decoding human cytomegalovirus. *Science*. 338:1088–1093. <https://doi.org/10.1126/science.1227919>
- Sylwester, A.W., B.L. Mitchell, J.B. Edgar, C. Taormina, C. Pelte, F. Ruchti, P.R. Sleath, K.H. Grabstein, N.A. Hosken, F. Kern, et al. 2005. Broadly targeted human cytomegalovirus-specific CD4+ and CD8+ T cells dominate the memory compartments of exposed subjects. *J. Exp. Med.* 202: 673–685. <https://doi.org/10.1084/jem.20050882>
- Ternette, N., H. Yang, T. Partridge, A. Llano, S. Cedeño, R. Fischer, P.D. Charles, N.L. Dudek, B. Mothe, M. Crespo, et al. 2016. Defining the HLA class I-associated viral antigen repertoire from HIV-1-infected human cells. *Eur. J. Immunol.* 46:60–69. <https://doi.org/10.1002/eji.201545890>
- Vescovini, R., C. Biasini, F.F. Fagnoni, A.R. Telera, L. Zanlari, M. Pedrazzoni, L. Bucci, D. Monti, M.C. Medici, C. Chezzi, et al. 2007. Massive load of functional effector CD4+ and CD8+ T cells against cytomegalovirus in very old subjects. *J. Immunol.* 179:4283–4291. <https://doi.org/10.4049/jimmunol.179.6.4283>
- Wagner, M., A. Gutermann, J. Podlech, M.J. Reddehase, and U.H. Koszinowski. 2002. Major histocompatibility complex class I allele-specific cooperative and competitive interactions between immune evasion proteins of cytomegalovirus. *J. Exp. Med.* 196:805–816. <https://doi.org/10.1084/jem.20020811>
- Weekes, M.P., P. Tomasec, E.L. Huttlin, C.A. Fielding, D. Nusinow, R.J. Stanton, E.C. Wang, R. Aicheler, I. Murrell, G.W. Wilkinson, et al. 2014. Quantitative temporal viromics: an approach to investigate host-pathogen interaction. *Cell*. 157:1460–1472. <https://doi.org/10.1016/j.cell.2014.04.028>
- Weekes, M.P., M.R. Wills, K. Mynard, A.J. Carmichael, and J.G. Sissons. 1999. The memory cytotoxic T-lymphocyte (CTL) response to human cytomegalovirus infection contains individual peptide-specific CTL clones that have undergone extensive expansion in vivo. *J. Virol.* 73:2099–2108.
- Wiertz, E.J., T.R. Jones, L. Sun, M. Bogoy, H.J. Geuze, and H.L. Ploegh. 1996a. The human cytomegalovirus US11 gene product dislocates MHC class I heavy chains from the endoplasmic reticulum to the cytosol. *Cell*. 84: 769–779. [https://doi.org/10.1016/S0092-8674\(00\)81054-5](https://doi.org/10.1016/S0092-8674(00)81054-5)
- Wiertz, E.J., D. Tortorella, M. Bogoy, J. Yu, W. Mothes, T.R. Jones, T.A. Rapoport, and H.L. Ploegh. 1996b. Sec61-mediated transfer of a membrane protein from the endoplasmic reticulum to the proteasome for destruction. *Nature*. 384:432–438. <https://doi.org/10.1038/384432a0>
- Wills, M.R., A.J. Carmichael, K. Mynard, X. Jin, M.P. Weekes, B. Plachter, and J.G. Sissons. 1996. The human cytotoxic T-lymphocyte (CTL) response to cytomegalovirus is dominated by structural protein pp65: frequency, specificity, and T-cell receptor usage of pp65-specific CTL. *J. Virol.* 70: 7569–7579.
- Wölfl, M., A. Rutebemberwa, T. Mosbrugger, Q. Mao, H.M. Li, D. Netski, S.C. Ray, D. Pardoll, J. Sidney, A. Sette, et al. 2008. Hepatitis C virus immune escape via exploitation of a hole in the T cell repertoire. *J. Immunol.* 181: 6435–6446. <https://doi.org/10.4049/jimmunol.181.9.6435>
- Zhou, Y.F., M.B. Leon, M.A. Waclawiw, J.J. Popma, Z.X. Yu, T. Finkel, and S.E. Epstein. 1996. Association between prior cytomegalovirus infection and the risk of restenosis after coronary atherectomy. *N. Engl. J. Med.* 335: 624–630. <https://doi.org/10.1056/NEJM199608293350903>
- Zimmermann, C., D. Kowalewski, L. Bauersfeld, A. Hildenbrand, C. Gerke, M. Schwarzmüller, V.T.K. Le-Trilling, S. Stevanovic, H. Hengel, F. Momberg, and A. Halenius. 2019. HLA-B locus products resist degradation by the human cytomegalovirus immunoevasin US11. *PLoS Pathog.* 15: e1008040. <https://doi.org/10.1371/journal.ppat.1008040>

## Supplemental material

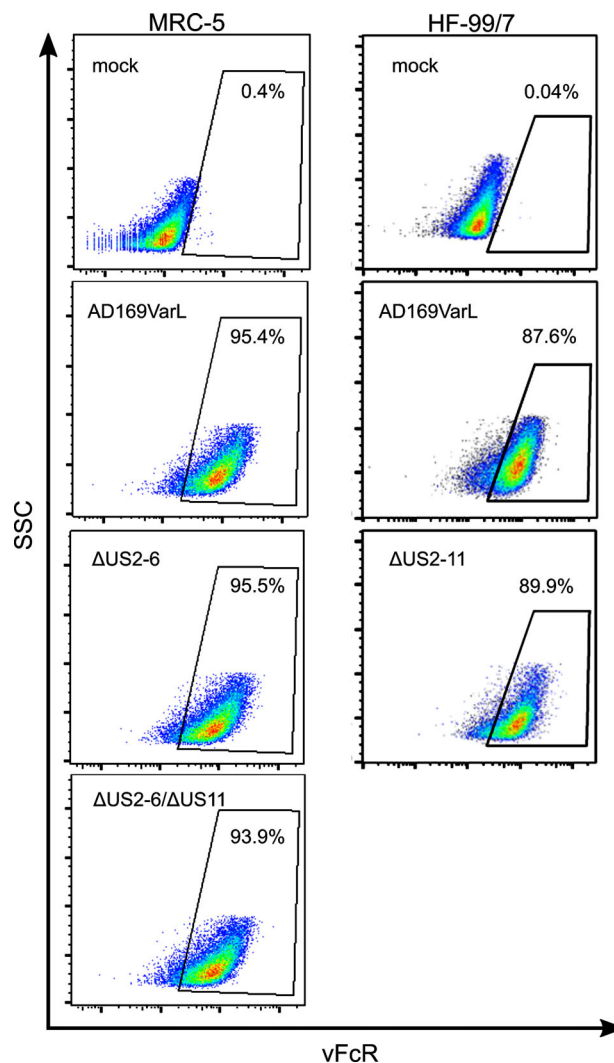
Lübke et al., <https://doi.org/10.1084/jem.20191164>

Figure S1. **Flow cytometry-based determination of the infection rate.** Cells were permeabilized and treated with Fc-FITC, which binds to the HCMV-encoded Fc-receptor (vFcR). Infection rate was determined once per infection experiment. SSC, side scatter.

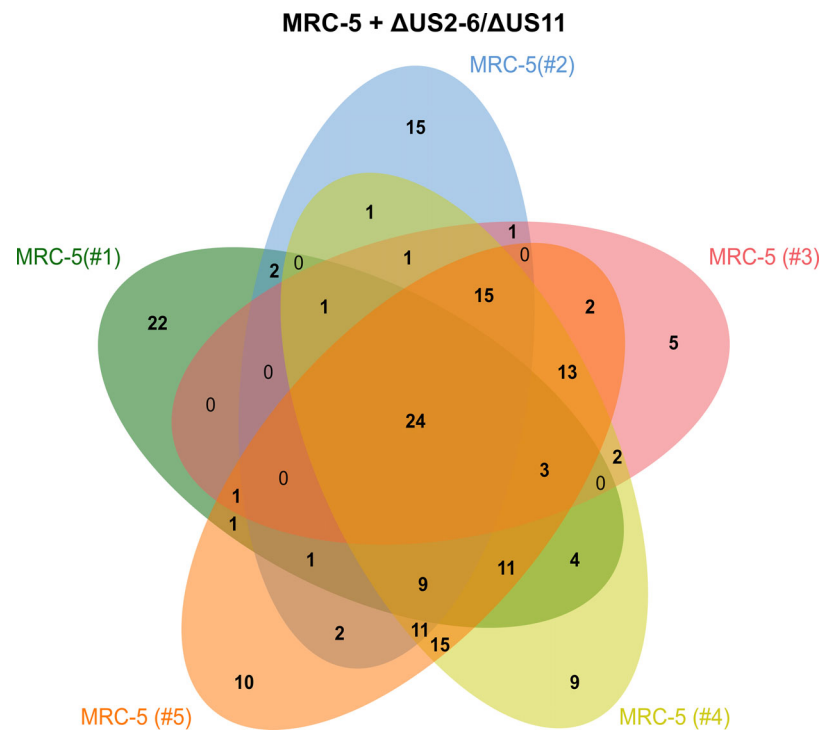


Figure S2. **Overlap analysis of HCMV-derived HLA ligands between five independent HLA ligand elutions from MRC-5 cells infected with AD169  $\Delta$ US2-6/ $\Delta$ US11.**



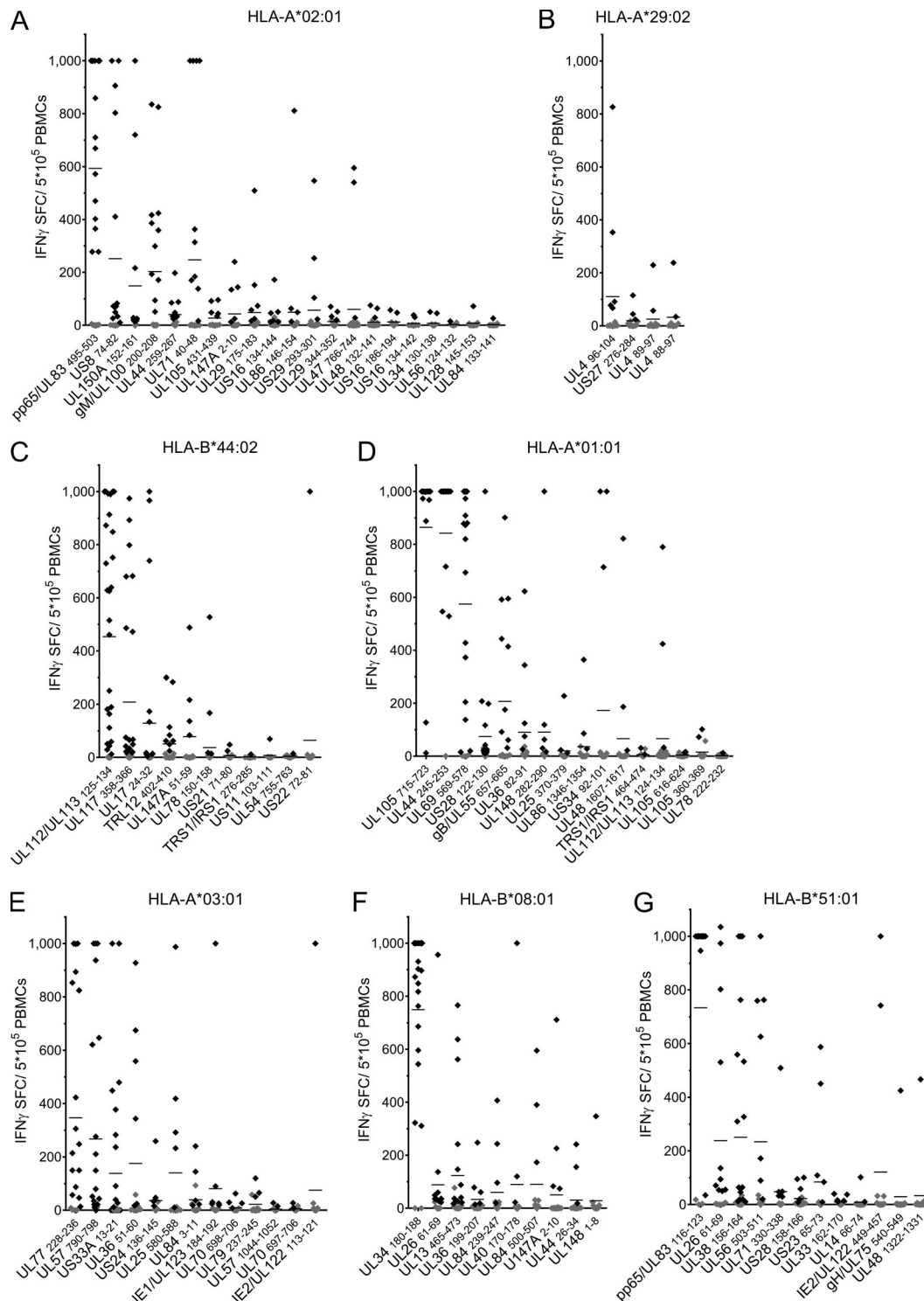


Figure S3. **Results of ELISpot screening. (A–G)** ELISpot screening of positively tested peptides with HLA-A\*02:01 (A), HLA-A\*29:02 (B), HLA-B\*44:02 (C), HLA-A\*01:01 (D), HLA-A\*03:01 (E), HLA-B\*08:01 (F), and HLA-B\*51:01 (G) restriction. Depicted are numbers of IFN $\gamma$  SFCs for each tested donor minus the spot numbers of the negative control of the respective donor. Positive evaluated donors are depicted in black, and negative tested donors in gray. Epitopes were tested once in 9–38 different HLA-matched donor PBMCs.

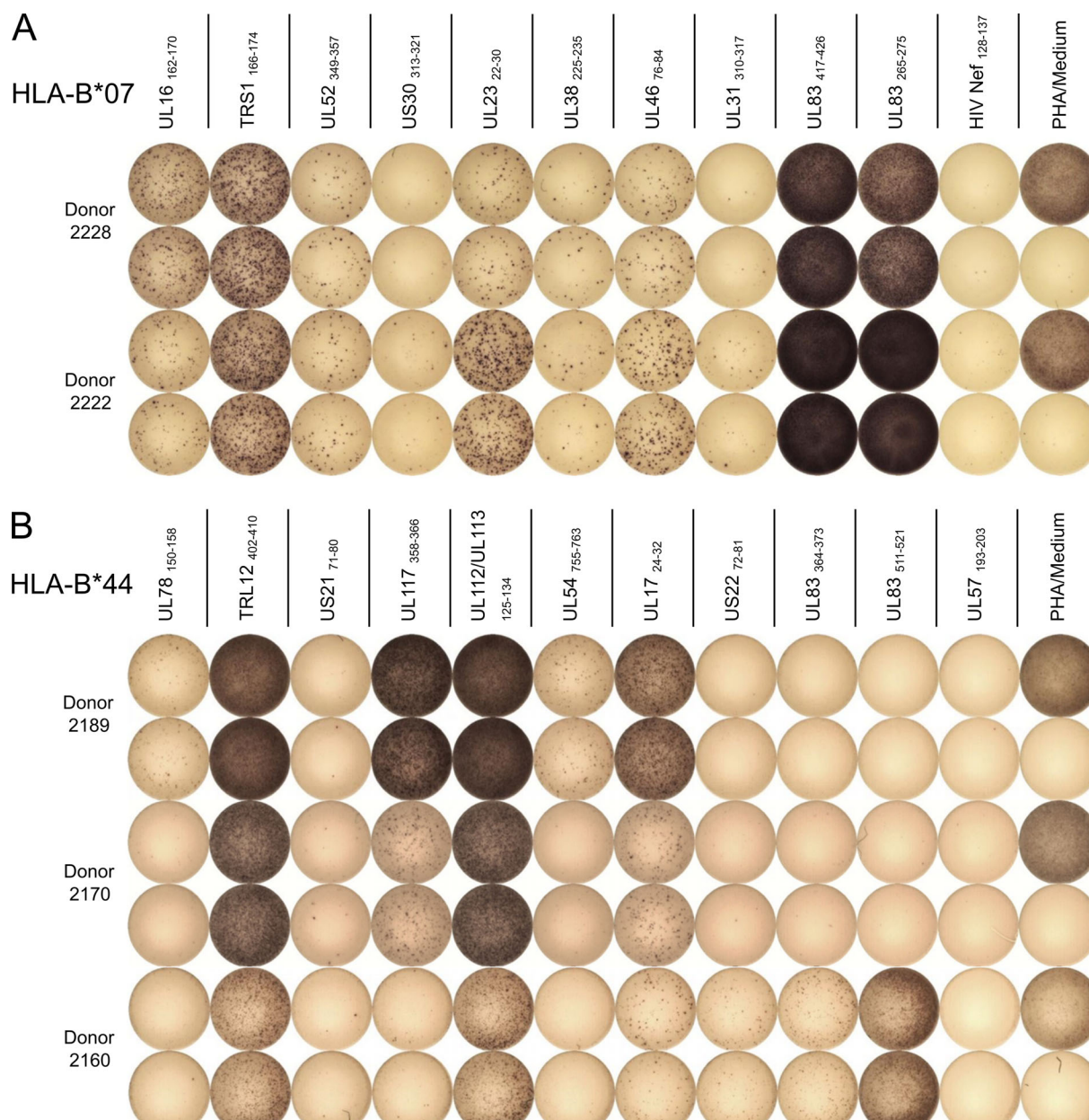


Figure S4. **Parallel recognition of multiple HCMV epitopes. (A and B)** Exemplary ELISpot results after 12-d amplification with HLA-B\*07-restricted (A) and HLA-B\*44-restricted (B) epitopes using PBMCs of two and three donors, respectively. PBMCs were stimulated with 10 novel and already known epitopes (columns 1–10). **(A)** pp65/UL83<sub>265–275</sub> (RPHERNGFTVL, column 10) is a previously identified epitope that was not contained in the ligands identified here. HIV Nef<sub>128–137</sub> (TPGPGVRYPL) and medium served as negative controls, and PHA as positive control. Representative results of two independent experiments. **(B)** pp65/UL83<sub>364–373</sub> (SEHPTFTSQY) and pp65/UL83<sub>511–521</sub> (QEFFWDANDIY) are already known epitopes that were not found as ligands in this study. UL57<sub>193–203</sub> (EEIPASDDVLF) served as negative control. Representative results of two independent experiments.

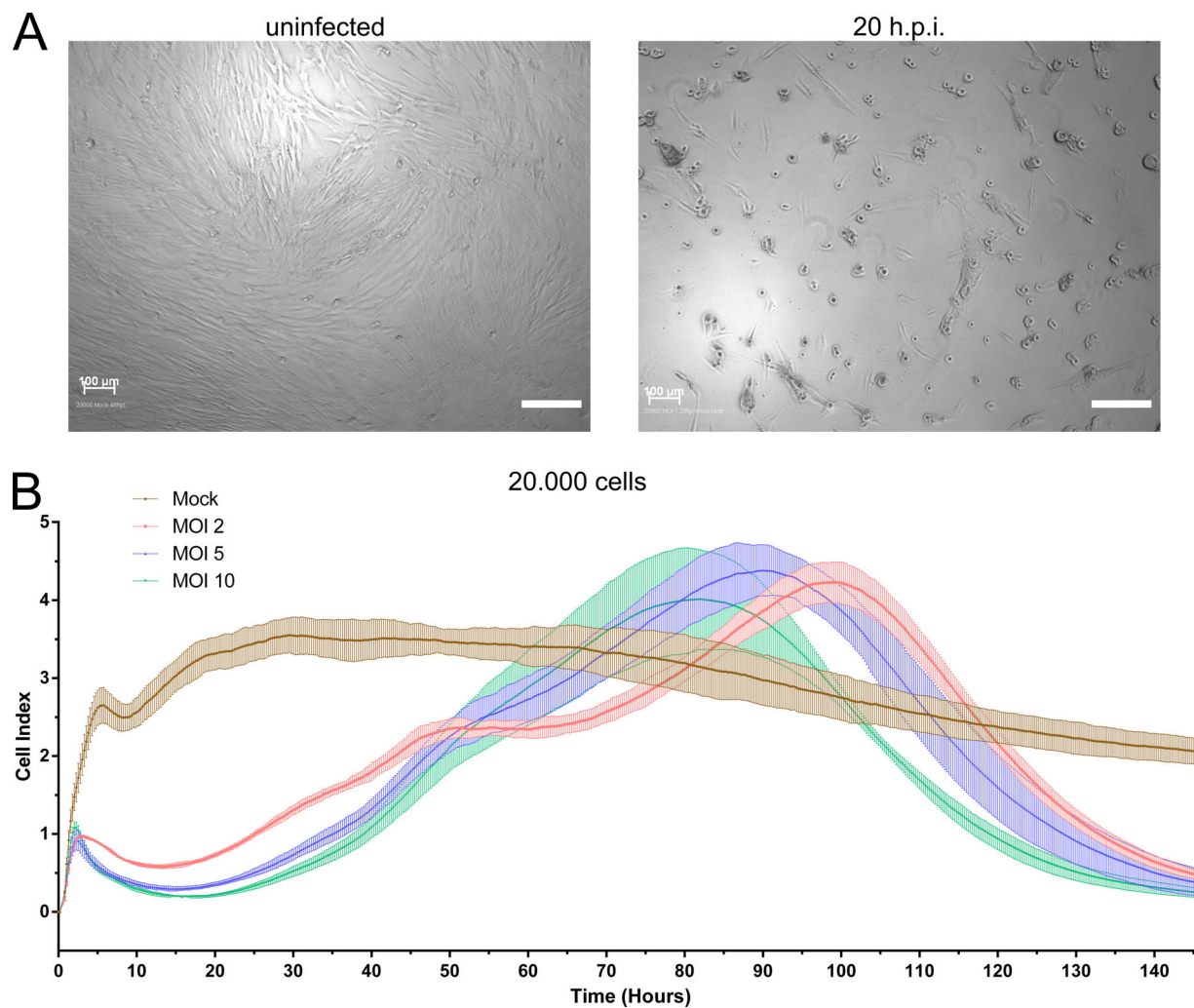


Figure S5. **Infection of MRC-5 cells with AD169  $\Delta$ US2-6 for following cytotoxicity testing of peptide-specific T cell clones.** **(A)** Comparison of morphology of uninfected and infected (20 h.p.i., MOI 1) MRC-5 cells. Scale bars, 200  $\mu$ m. **(B)** Titration of MOIs in comparison with mock-treated MRC-5 cells for the xCELLigence system. 20,000 cells/well of infected or mock-treated MRC-5 cells were seeded into 96-well E-plates. Impedance was measured every 15 min and normalized to impedance of wells with medium only. The resulting dimensionless normalized cell index indicates the changes in impedance normalized to  $t_0$ . Experiment was performed in triplicate. Shown are representative results of three independent experiments.

Table S1. T cell epitopes

ID	Position	Sequence	Tested HLA	Actual HLA restriction	ELISpot response rate (%)		Intracellular staining	Tetramer staining
					12-d stimulation	Ex vivo <sup>a</sup>		
MRC-5								
UL83 <sub>495-503</sub>	495-503	NLVPMVATV <sup>b</sup>	A*02:01	A*02:01	21/28 (75.0)	100.0	CD8	Positive
US8 <sub>74-82</sub>	74-82	GVLDAVWRV	A*02:01	A*02:01	13/18 (72.2)	50.0	CD8	Positive
UL150A <sub>152-161</sub>	152-161	ALWDVALLEV	A*02:01	A*02:01	10/14 (71.4)	25.0	CD8	Positive
UL100 <sub>200-208</sub>	200-208	TLIVNLVEV	A*02:01	A*02:01	11/20 (55.0)	25.0	CD8	Positive
UL44 <sub>259-267</sub>	259-267	GLFAVENFL	A*02:01	DR	7/13 (53.9)	0.0	CD4	nt
UL71 <sub>40-48</sub>	40-48	FLDENFKQL	A*02:01	DR	10/21 (47.6)	37.5	CD4	Negative
UL105 <sub>431-439</sub>	431-439	RLFDLPVYC	A*02:01		5/12 (41.7)	nt	nt	nt
UL147A <sub>2-10</sub>	2-10	SLFYRAVAL	A*02:01		5/13 (38.5)	12.5	nt	nt
UL29 <sub>175-183</sub>	175-183	RLQPNVPLV	A*02:01		6/18 (33.3)	0.0	nt	nt
US16 <sub>134-144</sub>	134-144	GLLAHIPALGV	A*02:01		6/22 (27.3)	0.0	nt	nt
US29 <sub>293-301</sub>	293-301	ALSPSTSKV	A*02:01		4/17 (23.5)	nt	nt	nt
UL29 <sub>344-352</sub>	344-352	SLYEANPEL	A*02:01		4/17 (23.5)	nt	nt	nt
UL86 <sub>146-154</sub>	146-154	TILDKILNV	A*02:01		4/20 (20.0)	nt	nt	nt
US16 <sub>186-194</sub>	186-194	TLINGVWVV	A*02:01		2/11 (18.2)	nt	nt	nt
US16 <sub>134-142</sub>	134-142	GLLAHIPAL	A*02:01		2/11 (18.2)	nt	nt	nt
UL48 <sub>132-141</sub>	132-141	ALYPEYITV	A*02:01		3/18 (16.7)	nt	nt	nt
UL47 <sub>766-744</sub>	766-774	GLNERLLSV	A*02:01		3/20 (15.0)	nt	nt	nt
UL34 <sub>130-138</sub>	130-138	ALFNQLVFTA	A*02:01		2/15 (13.3)	nt	nt	nt
UL56 <sub>124-132</sub>	124-132	FTDNVRFSV	A*02:01		1/13 (7.8)	nt	nt	nt
UL128 <sub>145-153</sub>	145-153	GLDQYLESV	A*02:01		1/13 (7.8)	nt	nt	nt
UL84 <sub>133-141</sub>	133-141	ALLGRLYFI	A*02:01		1/15 (6.7)	nt	nt	nt
UL4 <sub>96-104</sub>	96-104	NYNEQHYRY	A*29:02		5/13 (38.5)	nt	nt	nt
US27 <sub>276-284</sub>	276-284	LYVGQFLAY	A*29:02		3/12 (25.0)	nt	nt	nt
UL4 <sub>88-97</sub>	88-97	SFFPKLQGNV	A*29:02		2/9 (22.2)	nt	nt	nt
UL4 <sub>89-97</sub>	89-97	FFPKLQGNV	A*29:02		2/12 (16.7)	nt	nt	nt
UL16 <sub>162-170</sub>	162-170	YPRPPGSGL <sup>c</sup>	B*07:02	B*07:02	19/22 (86.4)	25.0	Negative	Positive
UL83 <sub>417-426</sub>	417-426	TPRVTGGGAM <sup>d</sup>	B*07:02	B*07:02	31/38 (81.6)	100.0	CD8	Positive
TRS1 <sub>166-174</sub>	166-174	SPRDAWIVL	B*07:02	B*07:02	15/22 (68.2)	20.0	CD8	Positive
UL52 <sub>349-357</sub>	349-357	SPSRDRFVQL	B*07:02	B*07:02	14/21 (66.7)	33.3	Negative	Positive
UL23 <sub>22-30</sub>	22-30	RPWKPGQRV	B*07:02	B*07:02	15/28 (53.6)	66.7	CD8	Positive
UL46 <sub>76-84</sub>	76-84	SPRHLIYSL	B*07:02	B*07:02	11/22 (50.0)	0.0	CD4/CD8	Positive
UL38 <sub>225-235</sub>	225-235	IPMTFVDRDSL	B*07:02		5/14 (35.7)	nt	nt	nt
US30 <sub>313-321</sub>	313-321	RPFPTHQL	B*07:02		4/13 (30.8)	0.0	nt	nt
UL83 <sub>49-57</sub>	49-57	RVSQPSLIL	B*07:02		4/15 (26.7)	nt	nt	nt
UL34 <sub>180-188</sub>	180-188	LPHERHREL	B*07:02		3/12 (25.0)	nt	nt	nt
UL82 <sub>245-254</sub>	245-254	SPHPPTSVFL	B*07:02		3/12 (25.0)	nt	nt	nt
UL27 <sub>485-493</sub>	485-493	IPDYRSVSL	B*07:02		4/18 (22.2)	nt	nt	nt
UL31 <sub>310-317</sub>	310-317	APFGRVSV	B*07:02		3/15 (20.0)	nt	nt	nt
TRS1/IRS1 <sub>92-99</sub>	92-99	IPVERQAL	B*07:02		2/12 (16.7)	nt	nt	nt
UL98 <sub>135-143</sub>	135-143	APNYRQVEL	B*07:02		2/12 (16.7)	nt	nt	nt
UL40 <sub>210-218</sub>	210-218	LPNDHHYAL	B*07:02		1/17 (5.9)	nt	nt	nt
US12 <sub>82-89</sub>	82-89	APYLRDTL	B*07:02		1/19 (5.3)	nt	nt	nt



Table S1. T cell epitopes (Continued)

ID	Position	Sequence	Tested HLA	Actual HLA restriction	ELISpot response rate (%)		Intracellular staining	Tetramer staining
					12-d stimulation	Ex vivo <sup>a</sup>		
UL112/ UL113 <sub>125–134</sub>	125–134	SEGNLQVTY	B*44:02	B*44:02	26/31 (83.9)	62.5	CD8	Positive
UL117 <sub>358–366</sub>	358–366	HETGVYQMW	B*44:02	B*44:02	17/26 (65.4)	62.5	CD8	Positive
UL17 <sub>24–32</sub>	24–32	DEQVSKRSW	B*44:02	B*44:02	11/24 (45.8)	12.5	CD8	Positive
TRL12 <sub>402–410</sub>	402–410	SESEFIVRY	B*44:02	B*44:02	8/20 (40.0)	37.5	CD8	Positive
UL147A <sub>51–59</sub>	51–59	EEQDYRALL	B*44:02		4/12 (33.3)	nt	nt	nt
UL78 <sub>150–158</sub>	150–158	RENAGVALY	B*44:02		4/21 (19.1)	nt	nt	nt
US21 <sub>71–80</sub>	71–80	AEPNFPKNVW	B*44:02		2/14 (14.3)	nt	nt	nt
TRS1/IRS1 <sub>276–285</sub>	276–285	EEATALGREL	B*44:02		1/10 (10.0)	nt	nt	nt
US11 <sub>103–111</sub>	103–111	SESLVAKRY	B*44:02		1/10 (10.0)	nt	nt	nt
UL54 <sub>755–763</sub>	755–763	LENGVTHRF	B*44:02		1/14 (7.1)	nt	nt	nt
US22 <sub>72–81</sub>	72–81	REQAAIPQIY	B*44:02		1/16 (6.3)	nt	nt	nt
UL57 <sub>640–648</sub>	640–648	FVDDEALGF	C*05:01		2/11 (18.2)	nt	nt	nt
<b>HF-99/7</b>								
UL105 <sub>715–723</sub>	715–723	YADPFLKY <sup>e</sup>	A*01:01	A*01:01	15/15 (100.0)	90.9	CD8	Positive
UL44 <sub>245–253</sub>	245–253	VTEHDTLLY <sup>c</sup>	A*01:01	A*01:01	13/14 (92.9)	100.0	CD8	Positive
UL69 <sub>569–578</sub>	569–578	RTDPATLTAY	A*01:01	A*01:01	19/23 (82.6)	66.7	CD8	Positive
US28 <sub>122–130</sub>	122–130	ITEIALDRY	A*01:01	A*01:01	14/24 (58.3)	14.3	CD8	Positive
UL55 <sub>657–665</sub>	657–666	NTDFRVLELY	A*01:01	A*01:01	9/16 (56.3)	0.0	CD8	Positive
UL36 <sub>82–91</sub>	82–91	FVEGPGFMRY	A*01:01		5/14 (35.7)		nt	nt
UL148 <sub>282–290</sub>	282–290	SLDRFIVQY	A*01:01	DR	5/14 (35.7)		CD4	nt
UL25 <sub>370–379</sub>	370–379	YTSRGALYLY	A*01:01		3/14 (21.4)		nt	nt
UL86 <sub>1346–1354</sub>	1,346–1,354	TSETHFGNY	A*01:01		3/15 (20.0)		nt	nt
US34 <sub>92–101</sub>	92–101	GSDALPAGLY	A*01:01		3/16 (18.8)		nt	nt
UL48 <sub>1607–1617</sub>	1,607–1,617	VTDYGNVAFKY	A*01:01		3/16 (18.8)		nt	nt
IRS1/TRS1 <sub>464–474</sub>	464–474	LLDELGAVFGY	A*01:01		2/13 (15.4)		nt	nt
UL112/ UL113 <sub>124–134</sub>	124–134	ISEGNLQVTY	A*01:01		3/20 (15.0)		nt	nt
UL105 <sub>616–624</sub>	916–924	VTDPPEHMM	A*01:01		2/14 (14.3)		nt	nt
UL105 <sub>360–369</sub>	360–369	DLDFGDLKY	A*01:01		2/16 (12.5)		nt	nt
UL78 <sub>222–232</sub>	222–232	YSRRDHVWSY	A*01:01		1/16 (6.3)		nt	nt
UL77 <sub>228–236</sub>	228–236	GLYTQPRWK	A*03:01	A*03:01	16/21 (76.2)	50.0	CD8	Positive
UL57 <sub>790–798</sub>	790–798	RVKNRPIYR	A*03:01	A*03:01	14/23 (60.9)	33.3	CD8	Positive
UL36 <sub>51–60</sub>	51–60	RSALGPFVGK	A*03:01	A*03:01	6/15 (40.0)		CD8	Positive
UL123 <sub>184–192</sub>	184–192	KLGGALQAK <sup>f</sup>	A*03:01		6/15 (40.0)		nt	nt
US33A <sub>13–21</sub>	13–21	KLGYRPHAK	A*03:01	A*03:01	11/29 (37.9)		CD8	Positive
US24 <sub>136–145</sub>	136–145	RVYAYDTREK	A*03:01		4/11 (36.4)		nt	nt

Table S1. T cell epitopes (Continued)

ID	Position	Sequence	Tested HLA	Actual HLA restriction	ELISpot response rate (%)		Intracellular staining	Tetramer staining
					12-d stimulation	Ex vivo <sup>a</sup>		
UL25 <sub>580–588</sub>	580–588	GVSSVTLLK	A*03:01		5/14 (35.7)		nt	nt
UL84 <sub>3–11</sub>	3–11	RVDPNLRNR	A*03:01		5/15 (33.3)		nt	nt
UL70 <sub>698–706</sub>	698–706	SVRLPYMYK	A*03:01		4/16 (25.0)		nt	nt
UL79 <sub>237–245</sub>	237–245	RTFAGTLSR	A*03:01		3/14 (21.4)		nt	nt
UL57 <sub>1044–1052</sub>	1,044–1,052	RLADVLIKR	A*03:01		2/13 (15.4)		nt	nt
UL70 <sub>697–706</sub>	697–706	RSVRLPYMYK	A*03:01		2/15 (13.3)		nt	nt
UL122 <sub>113–121</sub>	113–121	SVSSAPLNK	A*03:01		1/14 (7.1)		nt	nt
UL34 <sub>180–188</sub>	180–188	LPHRHREL	B*08:01	B*08:01	20/22 (90.9)	85.7	CD8	Positive
UL26 <sub>61–69</sub>	61–69	LPYPRGYTL	B*08:01	B*08:01/ B*51:01	11/16 (68.8)	16.7	CD8	Positive
UL13 <sub>465–473</sub>	465–473	YLVRRPMTI	B*08:01	B*08:01	11/22 (50.0)	33.3	Negative	Positive
UL36 <sub>199–207</sub>	199–207	VMKFKETSF	B*08:01		5/13 (38.5)		nt	nt
UL84 <sub>239–247</sub>	239–247	TPLLKRLPL	B*08:01		4/14 (28.6)		nt	nt
UL40 <sub>170–178</sub>	170–178	HLKLRPATF	B*08:01		3/13 (23.1)		nt	nt
UL84 <sub>500–507</sub>	500–507	FISSKHTL	B*08:01		3/14 (21.4)		nt	nt
UL147A <sub>2–10</sub>	2–10	SLFYRAVAL	B*08:01		4/22 (18.2)		nt	nt
UL44 <sub>26–34</sub>	26–34	QLRSVIRAL	B*08:01		2/14 (14.3)		nt	nt
UL148 <sub>1–8</sub>	1–8	MLRLFTL	B*08:01		1/14 (7.1)		nt	nt
UL83 <sub>116–123</sub>	116–123	LPLKMLNI <sup>g</sup>	B*51:01	B*51:01	12/15 (80.0)	87.5	CD8	Positive
UL38 <sub>156–164</sub>	156–164	FPVEVRSHV	B*51:01	B*51:01	15/23 (65.2)	0.0	CD8	Positive
UL26 <sub>61–69</sub>	61–69	LPYPRGYTL	B*51:01	B*08:01/B*51:01	10/16 (62.5)	33.3	CD8	Positive
UL56 <sub>503–511</sub>	503–511	DARSRIHNV	B*51:01	B*51:01	8/15 (53.3)		CD8	Positive
UL71 <sub>330–338</sub>	330–338	IPPPQIPFV	B*51:01		6/15 (40.0)		nt	nt
US28 <sub>158–166</sub>	158–166	IAIPHFMMV	B*51:01		5/15 (33.3)		nt	nt
US23 <sub>65–73</sub>	65–73	IPHNWFLQV	B*51:01		5/15 (33.3)		nt	nt
UL33 <sub>162–170</sub>	162–170	VPAAVYTTV	B*51:01		5/15 (33.3)		nt	nt
UL14 <sub>66–74</sub>	66–74	FPAHDWPEV	B*51:01		2/15 (13.3)		nt	nt
UL122 <sub>449–457</sub>	449–457	MPVTHPPEV	B*51:01		2/15 (13.3)		nt	nt
UL75 <sub>540–549</sub>	540–549	FPDATVPATV	B*51:01		1/15 (6.7)		nt	nt
UL48 <sub>1322–1331</sub>	1,322–1,331	LPYLSAERTV	B*51:01		1/15 (6.7)		nt	nt
UL78 <sub>335–343</sub>	335–343	KRAMYSVEL	C*07:01		2/15 (13.3)		nt	nt

nt, not tested.

<sup>a</sup>Ex vivo ELISpot assays were performed using donors that were positively tested in ELISpot assays with prior 12 d stimulation.<sup>b</sup>Diamond et al. (1997).<sup>c</sup>Elkington et al. (2003).<sup>d</sup>Weekes et al. (1999).<sup>e</sup>Kim et al. (2011).<sup>f</sup>Braendstrup et al. (2014).<sup>g</sup>Nastke et al. (2005).

Table S2 and Datasets S1–S3 are provided online as separate Excel (Table S2, Dataset S1, and Dataset S3) and PDF (Dataset S2) files. Table S2 lists positions of dominant epitopes within whole proteome prediction. Dataset S1 lists HLA ligands identified from extracts of MRC-5 cells. Dataset S2 shows a comparison of annotated fragment spectra of 50 randomly selected HCMV-derived HLA ligand identifications with their synthetic counterparts. Spectral pairs found to be mismatching in manual evaluation based on missing fragment ions in the natural spectrum or mismatching intensity distributions are outlined in red. Dataset S3 lists HLA ligands identified from extracts of HF-99/7 cells.

## References

- Braendstrup, P., B.K. Mortensen, S. Justesen, T. Osterby, M. Rasmussen, A.M. Hansen, C.B. Christiansen, M.B. Hansen, M. Nielsen, L. Vindeløv, et al. 2014. Identification and HLA-tetramer-validation of human CD4+ and CD8+ T cell responses against HCMV proteins IE1 and IE2. *PLoS One*. 9:e94892. <https://doi.org/10.1371/journal.pone.0094892>
- Diamond, D.J., J. York, J.Y. Sun, C.L. Wright, and S.J. Forman. 1997. Development of a candidate HLA A\*0201 restricted peptide-based vaccine against human cytomegalovirus infection. *Blood*. 90:1751–1767. <https://doi.org/10.1182/blood.V90.5.1751>
- Elkington, R., S. Walker, T. Crough, M. Menzies, J. Tellam, M. Bharadwaj, and R. Khanna. 2003. Ex vivo profiling of CD8+-T-cell responses to human cytomegalovirus reveals broad and multispecific reactivities in healthy virus carriers. *J. Virol.* 77:5226–5240. <https://doi.org/10.1128/JVI.77.9.5226-5240.2003>
- Kim, S., S. Lee, J. Shin, Y. Kim, I. Evnouchidou, D. Kim, Y.K. Kim, Y.E. Kim, J.H. Ahn, S.R. Riddell, et al. 2011. Human cytomegalovirus microRNA miR-US4-1 inhibits CD8(+) T cell responses by targeting the aminopeptidase ERAP1. *Nat. Immunol.* 12:984–991. <https://doi.org/10.1038/ni.2097>
- Nastke, M.D., L. Herrgen, S. Walter, D. Wernet, H.G. Rammensee, and S. Stevanović. 2005. Major contribution of codominant CD8 and CD4 T cell epitopes to the human cytomegalovirus-specific T cell repertoire. *Cell. Mol. Life Sci.* 62:77–86. <https://doi.org/10.1007/s00018-004-4363-x>
- Weekes, M.P., M.R. Wills, K. Mynard, A.J. Carmichael, and J.G. Sissons. 1999. The memory cytotoxic T-lymphocyte (CTL) response to human cytomegalovirus infection contains individual peptide-specific CTL clones that have undergone extensive expansion in vivo. *J. Virol.* 73:2099–2108.